

Abundances and Kinematics of Field Halo and Disk Stars I: Observational Data and Abundance Analysis

Jon P. Fulbright^{1,2}
UCO/Lick Observatory, Dept of Astronomy, University of California, Santa Cruz, CA 95064

Received _____; accepted _____

arXiv:astro-ph/0006260v1 19 Jun 2000

¹Present address: Dominion Astrophysical Observatory, Herzberg Institute of Astrophysics, National Research Council, 5071 West Saanich Road, Victoria, BC V8X 4M6, Canada

²Email: Jon.Fulbright@nrc.ca

ABSTRACT

We describe observations and abundance analysis of a high-resolution, high-S/N survey of 168 stars, most of which are metal-poor dwarfs. We follow a self-consistent LTE analysis technique to determine the stellar parameters and abundances, and estimate the effects of random and systematic uncertainties on the resulting abundances. Element-to-iron ratios are derived for key alpha, odd, Fe-peak, r- and s-process elements. Effects of Non-LTE on the analysis of Fe I lines are shown to be very small on the average. Spectroscopically determined surface gravities are derived that are quite close to those obtained from Hipparcos parallaxes.

1. Introduction

The traditional explanation for the chemical evolution of the Galactic halo was put forth by Tinsley (1979) and is based on the differing products of the two main types of supernovae. Type Ia supernovae produce mainly Fe-group elements, while Type II supernovae produce lighter elements (including the so-called ‘alpha’ elements) as well as some Fe-group and heavier elements. Since the time between star formation and explosion differs between the two types (Type II need $\sim 10^7$ years, while Type Ia need $> 10^9$ years), there is a time in which the enrichment is from Type II SN. The stars created out of the ashes of these early Type II supernovae will be relatively rich in the alpha (and other light) elements until enough Type Ia supernovae can explode to ‘dilute’ the light elements with Fe-group elements. This overall pattern is seen observations of halo stars and clusters (see Wheeler *et al.* 1989 and McWilliam 1997 for reviews), and indicates that element ratios can be used as an indicator of the history of a stellar population.

Recent developments have shown that the chemical evolution of the halo is more complicated than the original Tinsley (1979) model. Nissen & Schuster (1997) studied stars of intermediate metallicity ($-1.3 < [\text{Fe}/\text{H}] < -0.5$) and found that there was a number of stars on halo-like orbits that exhibited significantly lower $[\alpha/\text{Fe}]$ ratios than the disk stars at similar metallicities. King (1997) found solar-like $[\alpha/\text{Fe}]$ ratios in the metal-poor proper motion pair HD 134439/40, and Carney *et al.* (1997) found sub-solar $[\alpha/\text{Fe}]$ ratios in the even more metal-poor star BD +80 245.

From a suggestion in Nissen & Schuster (1997), Hanson *et al.* (1998) found that in a sample metal-poor halo giants, about a third of the stars on retrograde orbits showed low values of $[\text{Na}/\text{Fe}]$, compared to none of the stars on prograde orbits. Stephens (1999) followed a suggestion by Carney *et al.* (1997) to study stars on orbits with large apogalactic radii, but concluded that the abundance ratios of such stars were not significantly different than what is found in the rest of the halo population.

The above studies do indicate that some halo stars deviate from the traditional halo chemical evolution model. However, in all of the above works only a limited number of stars were observed, so it is not readily possible to understand the true distribution of element ratios in the halo. Similarly, systematic differences between abundance studies, due to differences in data quality, wavelength coverage, temperature scales, atomic data, model atmospheres, etc., make it difficult to combine the results from previous surveys to improve the situation.

With this in mind, we have conducted a self-consistent survey of metal-poor stars with the goals of determining the distribution of element ratios within the halo, finding potential relationships between stellar kinematics and these element ratios, and how these relationships relate to the early chemical evolution of the Galaxy.

In this paper, we analyse the elemental abundance ratios of a large sample of metal-poor stars using high-resolution, high-S/N spectra. In Section 2 we discuss the selection of target stars and the observations. Section 3 includes the process for selecting the absorption lines and line data as well as the measurement of the line strengths. In Section 4 we use the line data to determine the stellar parameters for the target stars and then compare the results to literature determinations. In Section 5, we use these parameters and the line strengths to determine the abundances of the elements and estimate the uncertainties of the resulting abundances, while in Section 6 we discuss the possibility of non-LTE effects on the analysis.

In following papers in this series will focus on the scientific interpretation of the results of this analysis. Paper II will describe the trends of the elements with respect to [Fe/H] and to each other, as well as exploring relationships between the stellar kinematics and abundances. Paper III will use the derived metallicities of nearby stars to examine the subdwarf distance scale. Descriptions of further research with this data set will be included in these papers.

2. Star Selection, Observations, and Reductions

2.1. Target List

Our target list was created from multiple literature sources, selecting for metallicity, membership in the Hipparcos catalog, and observational considerations. However, this list is subject to selection biases common between the source surveys. In particular, many of the source papers select stars by kinematical criteria, potentially ignoring metal-poor stars with small proper motions. Although using multiple source surveys with different selection techniques may help eliminate this problem, we make no claims that this work is without selection effects.

Several sources contain lists of [Fe/H] values determined by spectroscopic means and include: Cayrel *et al.* (1997), Carney *et al.* (1994), Bond (1980), Pilachowski *et al.* (1993), Beers & Sommer-Larsen (1995), Fuhrmann *et al.* 1995, and Cavallo *et al.* (1997). Other sources used here, based on multicolor photometry are Sandage & Fouts (1987), Schuster & Nissen (1988), Schuster *et al.* (1993) and Olsen (1994). Sandage & Fouts (1987) observed stars in UBV filters, and we used their calibration of the $\delta(U-B)$ index to estimate [Fe/H]. The other sources use *ubvy* photometry, and we use the calibration of Schuster & Nissen (1989) to convert to [Fe/H]. For all of the above sources, stars with reported [Fe/H] $\lesssim -0.8$ were placed on the preliminary target list. We also included a list of kinematically-selected stars from the Hipparcos catalog (ESA 1997) from Hanson (private communication) and several stars suggested by N. Reid (private communication) and R. Peterson (private communication). The final target list includes over 400 stars.

2.2. Observations and Data Reduction

The stellar spectra were obtained between August 1994 and May 1999. Table 1 gives the details of each run, and Table 2 lists the basic observational data on each star. Generally, the observations were taken at spectral resolution $R \sim 50000$, with a minimum S/N of 100 (per pixel). The S/N level at 5500 Å is listed in Table 2.

The majority of the data was obtained using the Shane 3-m telescope and the Hamilton spectrograph at Lick Observatory. In 1994 and 1995 the observations were obtained by M. Bolte, K. Wu, and M.

Shetrone. The 1994 runs used a 800x800 pixel CCD, which limited the wavelength coverage. Since that time a 2048x2048 CCD was used allowing full wavelength coverage. Data from the ESO 3.6-m and CASPEC spectrograph was kindly provided by M. Shetrone, who observed the stars during engineering time. The stars observed with the 10-m Keck 1 telescope and HIRES spectrograph (Vogt *et al.* 1994) in 1998 and 1999 were obtained during twilight, poor weather (in 1998) or between observation fields (in 1999).

Data reduction was done with the use of programs in the IRAF package ‘echelle’. The methods used are the same as those used in Fulbright & Kraft (1999). Only minor adjustments to the procedure were required to reduce the data obtained using spectrographs other than the Hamilton.

3. Line List and EW Measurements

3.1. Line Selection and gf-Values

A key problem in the analysis of stellar abundances is the need for quality atomic data. As the overall goal is to have the best possible abundance determinations, our guiding philosophy for line selection is to identify a set of self-consistent absorption lines that have high-quality relative gf-values and are easily measurable in the spectra of stars observed here (mainly metal-poor dwarfs).

The final line list is given in Table 3. Some of the gf-values have been altered from their original published values. The Fe I gf-values from the Oxford group have been increased by 0.04 dex, following a suggestion by McWilliam 1995. The Blackwell *et al.* (1980b) Fe II gf-values were calculated using a solar $\log \epsilon(\text{Fe}) = 7.67^3$. We therefore raised the gf-values by 0.15 dex to reflect our adopted solar Fe abundance, $\log \epsilon(\text{Fe}) = 7.52$. The Moity (1983) Fe II gf-values have been shifted by +0.11 dex to agree with the Blackwell *et al.* (1980b) scale. Poorly-performing lines from the references in Table 3 were eliminated through an empirical test involving 16 high-S/N spectra of well-studied stars. Consistently deviant, strong and/or blended lines were removed through an iterative process.

As an independent test, we measured the EWs of the line list in the two solar spectra taken in this survey. We then used the traditional solar parameters⁴ ($T_{\text{eff}} = 5770$ K, $\log g = 4.44$, $[\text{Fe}/\text{H}]_{\text{atm}} = 0$ and $\xi = 0.84$ km/s) to determine solar abundances. The results are exhibited in Table 4. As can be seen, we recreate the solar abundance ratios fairly well. The results of the analysis also improves between the lower-quality October 1998 spectra (S/N ~ 80) and higher-quality May 1999 spectra (S/N ~ 220). It should also be noted that most of the lines analyzed here are their strongest in the Sun, so the problems of damping and unknown blends should be the largest in the Sun.

Hyperfine splitting (hfs) effects were taken into account for the Li I and Na I D lines and the lines of Ba II and Eu II. We assumed solar system isotopic ratios for these elements. Other odd-z elemental lines were treated as single lines in this analysis.

Except for Ba, the Unsöld (1955) approximation was used to calculate the van der Waals damping constant. It was found that multiplying the damping constant by some factor generally decreased the T_{eff} obtained by the Fe I excitation potential plot significantly. As the weak lines used for the analysis generally did not show deviations from Gaussian profiles (see below), it was felt that these lines should

³In this paper, we define $\log \epsilon(X) = \log n(X) + 12.0$.

⁴We use $[\text{Fe}/\text{H}]_{\text{atm}}$ to designate the overall abundance of the input atmospheric model. As will be discussed later, this may not be the same as the derived iron abundance ratio of the star, $[\text{Fe}/\text{H}]$.

not be affected significantly by damping. For Ba, however, it was found that it was necessary to multiply the Unsold approximation by 5.0, as suggested by Gratton & Sneden (1994).

To test this assumption, we rederived the stellar parameters for eight dwarfs after eliminating all Fe lines stronger than 50 mÅ. For the most metal-poor stars, there was little, if any, effect. This was partially due to the small number of lines stronger than 50 mÅ measured in these stars. As the metallicity increased, there was a trend indicating a preference for slightly lower T_{eff} and $\log g$ values. For dwarfs with $[\text{Fe}/\text{H}] > -1.0$, the effect was to prefer T_{eff} values ~ 75 K cooler and surface gravities ~ 0.1 dex lower. This trend was smaller for stars with lower surface gravities. There was very little effect on $[\text{Fe}/\text{H}]_{\text{atm}}$ and no consistent effect on ξ .

3.2. EW Measurements

Equivalent widths were measured using the ‘splot’ program in the IRAF ‘echelle’ package. Generally Gaussian fitting was used to measure lines, as testing with ThAr lamp spectra showed that weak lines were well fit by Gaussian profiles. Direct integration was used for the stronger lines ($\text{EW} \gtrsim 100$ mÅ). Direct integration was also used when a line was known to be one affected by hfs.

Lines that were blended with telluric features, night sky emission lines or the wings of strong stellar lines were not measured, nor were very strong lines and lines near or on bad pixel regions. For most lines measured on most spectra with average S/N, those measurements with EWs $\gtrsim 10$ mÅ are thought to be reliable, although this limit varies depending on S/N, line placement with respect to the blaze, and local spectral contaminants.

In total, 41256 EWs for the 17 elemental species on 191 spectra were measured. For stars with multiple observations, a single EW list was created for the star by combining the EWs from each observation and was used in the determination of stellar parameters and abundances. Note that the EW measures for the individual observations were used in creating the line list (section 3.1), the EW comparisons (section 3.3) and the determination of uncertainties (section 5). These equivalent widths are not included in this publication, but are available electronically from the Astronomical Data Center (ADC).

3.3. EW Comparisons

Figure 1 compares EW measurements between seven stars observed at both Lick and McDonald. The stars were observed 18 times (11 times at Lick, 7 times at McDonald), yielding 443 common line measurements (counting multiple Lick observations independently). The average offset, $\langle \text{EW}_{\text{Ham}} - \text{EW}_{\text{McD}} \rangle = -0.6 \pm 0.2$ mÅ (sdm) is small.

The observations from ESO and Keck do not have any stars in common with any other observation run, so no such comparison is possible. However, many observations have been made of common stars between Keck and Lick, namely in the work of the Lick/McDonald group (Shetrone 1996, for example) and Johnson (1999). The comparisons made in these papers show that there is not a systematic difference in EWs obtained with these spectrographs. No known study linking the ESO CASPEC spectrograph with either the Hamilton, HIRES or Sandiford spectrographs could be found.

Figures 2(a)–(d) compare EW measurements for stars in common with other studies. In all four cases, the average offset is less than 1 mÅ. In Figure 2(c) there are about a dozen EWs for which the EWs from Nissen & Schuster (1997) are noticeably greater than those measured from this study. These EWs all come from the spectra of HIP 59750 (= HD 106516) taken at Lick in April 1999. The other EWs in

common for this star between the the Nissen & Schuster (1997) list match well. It is not believed that the different chip used in the April 1999 run is the cause of this effect. There were four stars in common between the April 1999 Lick run and the January 1999 McDonald run. If there was a sizable offset between these runs, it would show up in Figure 1, but only a few slightly weaker lines from HIP 59750 can be seen in the 40–80 mÅ range. These anomalous measurements were discarded when creating the final EW list for this star.

4. Stellar Parameters

4.1. Deriving the Parameters

The basic stellar parameters (T_{eff} , $\log g$, $[\text{Fe}/\text{H}]_{\text{atm}}$, and ξ) were determined using the Fe lines in the spectra. Before analysis, Fe lines stronger than $\log(EW/\lambda) = -4.80$ (~ 75 mÅ at 5000 Å) were eliminated from both the Fe I and Fe II lists. This limits the effects of damping on both line measurement and abundance analysis. There were strong-lined stars, however, in which it was necessary to use stronger lines in order to determine the parameters. Even in these cases the strongest Fe lines used were limited to ~ 100 mÅ.

We use the LTE abundance program MOOG (Snedden 1973) to derive all of the abundances and synthetic spectra in this study. We use Kurucz (<http://cfaku5.harvard.edu>) model atmospheres. These atmospheres were computed using solar abundance ratios and convective overshoot. For atmospheres between grid points, a program was used to interpolate the values of ρx , temperature, gas pressure, and electron density for each layer within the atmosphere.

Since the assumption of solar abundance ratios does not hold in metal-poor stars, the value of $[\text{Fe}/\text{H}]_{\text{atm}}$ was set slightly higher than the measured $[\text{Fe}/\text{H}]$ value for the star. This procedure is designed to simulate the increased supply of electrons ionized from the usual excess of alpha elements. These extra electrons contribute significantly to the H^- opacity in the atmospheres of these stars.

We set the stellar parameters using an iterative process. First, the microturbulent velocity (ξ) is adjusted so the iron abundance given by the strong Fe I lines is the same given by the weak lines. Then the value of T_{eff} is adjusted so the Fe I lines with high excitation potential (EP) give the same iron abundance as those with lower EPs. Finally, the value of $\log g$ is adjusted so the iron abundance given by the Fe I lines matches the iron abundance given by the Fe II lines (within ~ 0.03 dex in most cases). This process is iterative, with small changes being made to the parameters between each step.

As this is an iterative process, it is necessary to have a first estimate of the parameters. For T_{eff} , we used the color-based T_{eff} scales of Carney (1983). We gave preference to the $(V - K)$ relationship when the photometry was available. Otherwise we used the $(b - y)$ relationship from Carney (1983) or the $(B - V)$ tables given in Appendix B of Gray (1992).

We chose the initial value of $\log g$ using the photometric T_{eff} and the star’s Hipparcos parallax. For the stars here, the mass was taken to be $0.8M_{\odot}$, and the bolometric corrections were taken from Alonso *et al.* (1995) for the dwarfs and Worthy (private communication) for the giants. The uncertainty in $\log g$ from this method is dominated by the uncertainty in π , which means this method is only suitable for nearby stars with reliable parallaxes ($\sigma_{\pi}/\pi < 0.2$), i.e. dwarfs.

We set the initial value of $[\text{Fe}/\text{H}]_{\text{atm}}$ to slightly higher than the values given by the source papers, and the initial ξ was set to 1.2 km/s. The initial guesses of T_{eff} and $\log g$ plus the final adopted atmospheric parameters are listed in Table 5.

This procedure was adjusted for ~ 20 giants in this survey. Strong lines and molecular features in

several regions made it difficult to create a full set of reliable Fe I lines. In these cases, we exploited the known sensitivity of $[V/Fe]$ to changes in T_{eff} . This is similar to the method described in Ivans *et al.* (1999), where the authors find a change in a giant’s T_{eff} by 125 K would result in a change in the $[V/Fe]$ of ~ 0.3 dex. As an Fe-peak element, $[V/Fe]$ is expected to be close to solar over a wide range of metallicities. This value has been observed in globular cluster giants (see Ivans *et al.*), field giants (Johnson 1999) and dwarfs from this study.

In these giants, we first attempted to use the Fe lines to set the stellar parameters as above. When this was completed, if $[V/Fe] \sim 0$ (as was the case for stars with $\log g \gtrsim 2.0$), no further adjustments were made. Otherwise, we changed the value of T_{eff} as little as necessary to obtain $[V/Fe] \sim 0$ (usually upwards by ~ 75 – 125 K). The resulting compromise parameters usually left a slightly larger disagreement between Fe I and Fe II than was seen in dwarfs.

In the few giant stars in which no V lines could be measured, we used $[Ni/Fe]$ and $[Cr/Fe]$ in a similar way. However, both of these abundance ratios are less sensitive to T_{eff} than $[V/Fe]$, and the value of the $[Cr/Fe]$ ratio is known to decrease in very metal-poor stars (McWilliam 1997). Therefore $[Cr/Fe]$ was not used for giants with $[Fe/H] < -1.5$. Using these elements as backups was also helpful in the case of a few stars with strong V lines, as the effects of hyperfine splitting on V were not accounted for in this study.

Also included in the data analysis were the stars of Stephens (1999), as these high-velocity stars increase the number of stars on extreme orbits in this survey. The Keck-HIRES EWs from that paper were used with the line list in this study. For these stars the initial estimates for the stellar parameters were those given by Stephens (1999).

4.2. Comparison of Stellar Parameters to Literature Values

As a check of the parameters used here, we compare our values to those determined by other studies. Alonso *et al.* (1995) used the IR flux method (IRFM; Blackwell & Shallis (1977)) to determine the T_{eff} values for a number of stars. Figure 3(a) compares the 55 T_{eff} determinations common between the two studies. The average offset is $\langle T_{\text{eff}} - T_{\text{Alonso}} \rangle = -38 \pm 20$ (sdom). There does not seem to be a slope over the ~ 2000 K range for which common T_{eff} values are available.

Carney *et al.* (1994) also determined T_{eff} values for a large number of stars using photometric indexes. Figure 3(b) compares the 68 determinations in common. The average offset is $\langle T_{\text{eff}} - T_{\text{CLLA}} \rangle = -12 \pm 14$ K (sdom).

Figure 3(c) shows the comparisons between the T_{eff} values determined by $V - K$ and $b - y$ colors using the Carney (1983) relationships. The average offset for the $V - K$ colors is $\langle T_{\text{eff}} - T_{V-K} \rangle = +36 \pm 15$ K (sdom, $N = 105$), and for $b - y$ it is $\langle T_{\text{eff}} - T_{b-y} \rangle = +109 \pm 14$ K (sdom, $N = 140$). It should be noted that no reddening corrections were made before calculating T_{eff} , and the deviant points at $T_{\text{eff}} \lesssim 4500$ K are giants. For example, at $b - y = 0.50$ mag, an $E(b - y) = 0.05$ mag will decrease the photometric T_{eff} by 250 K. Another possible explanation may be that these relationships were derived to fit dwarfs, and differences in the atmospheres of giants (e.g., stronger lines for a given T_{eff}) could lead to changes in the T_{eff} -color relationship.

Figure 3(d) compares the T_{eff} values determined here against the published T_{eff} values from several studies. Overall, the other studies’ T_{eff} values seem to be ~ 50 – 100 K warmer.

Figures 4(a) and (b) compare the results of Gratton *et al.* (1996) against the parameter values derived in this study. Gratton *et al.* (1996) re-analyzed literature data using T_{eff} values derived from photometric

colors and $\log g$ values derived from ionization equilibrium. The mean offset in T_{eff} (this study – theirs) is -90 ± 19 K (sdom, $N = 66$), while the mean offset in $\log g$ is -0.22 ± 0.05 dex (sdom, $N = 66$). As seen with the comparisons to the Carney (1983) temperatures, the T_{eff} values we derive for cool giants ($T_{\text{eff}} \lesssim 4500$ K) are warmer than what was cited by Gratton *et al.* (1996). This is not seen when our T_{eff} values for giants are compared with those derived by others using similar spectroscopic techniques, (see Figure 3d), but is seen in the comparison to Carney (1983) photometric T_{eff} values. Therefore, we believe there is a systematic difference between the photometric and spectroscopic T_{eff} scales when applied to cool giants. These giants are also the ones in which the value of T_{eff} was adjusted to make $[V/\text{Fe}] \sim 0$, but the magnitude of the changes is smaller than the discrepancies seen.

The final comparison made here is between the value of $[\text{Fe}/\text{H}]$ determined in this study and the $[\text{m}/\text{H}]$ values presented in the Carney *et al.* (1994) survey (Figure 5). The latter were determined by chi-square fits of high-resolution, very low-S/N spectra to a grid of synthetic spectra. The average offset for the 83 points is $\langle [\text{Fe}/\text{H}] - [\text{m}/\text{H}] \rangle = +0.03 \pm 0.02$ dex (sdom, $N = 71$), which is surprisingly good agreement considering the different techniques employed.

5. Abundances and Error Analysis

With all of the necessary ingredients in place, it is now possible to calculate the abundances of the remaining elements. This was generally straightforward. The line data were analyzed by MOOG using the adopted atmosphere for that star. The MOOG routine ‘blends’ was used for analyzing lines affected by hyperfine splitting. For each star the final abundance for a given species was the straight mean of the individual lines.

To compute the ratios of the elements with respect to the Sun, we adopt the solar abundances of Anders & Grevesse (1989). The sole exception is Fe, for which we adopt $\log \epsilon(\text{Fe}) = 7.52$. The derived abundance ratios are given in Table 6. The $[\text{Fe}/\text{H}]$ given is derived from the mean of Fe I and Fe II. The $[\text{Ti}/\text{Fe}]$ given is also derived from the mean of Ti I and Ti II, except that the value of $\log \epsilon(\text{TiI})$ was increased by 0.11 dex. This offset was derived from the average difference between $\log \epsilon(\text{TiI})$ and $\log \epsilon(\text{TiII})$ for several stars with well-determined parameters and good Ti EW measurements. For example, from our observations of the solar spectrum, we derive $\log \epsilon(\text{TiI}) = 4.86$ and $\log \epsilon(\text{TiII}) = 5.00$ before the adjustment, while Anders & Grevesse (1989) give $\log \epsilon(\text{Ti}) = 4.99$.

The usually-measured Eu II lines were too weak to be measured in the extremely alpha-weak star BD +80 245 (= HIP 40068). As this star is very interesting, and the r-process element Eu is a clue to the history of this star, we used the Eu II lines given by Sneden *et al.* 1996. The Eu II lines and the measured EWs are: $\text{EW}(3819.67) = 2.4$ mÅ, $\text{EW}(3971.96) = 2.4$ mÅ, $\text{EW}(4129.72) = 1.0$ mÅ (upper limit), and $\text{EW}(4205.05) = 2.0$ mÅ. The resulting abundance is $[\text{Eu}/\text{Fe}] = -0.76 \pm 0.25$. Due to the extreme weakness of the lines, it may be best to consider this abundance a reliable upper limit.

Figures 6(a)–(c) illustrate the frequency functions of this study for T_{eff} , $\log g$ and $[\text{Fe}/\text{H}]$. As can be seen, the survey is dominated by dwarfs with solar-like T_{eff} values. The survey is split nearly evenly at $[\text{Fe}/\text{H}] = -1$, with 82 stars below and 86 stars above this value. The mean $[\text{Fe}/\text{H}]$ of the 168 stars observed in this survey is -1.21 . The minimum $[\text{Fe}/\text{H}]$ value is -3.01 from HIP 50173 (= HD 88609), and the maximum $[\text{Fe}/\text{H}]$ is $+0.02$ for the Sun.

5.1. Estimating the Internal Errors

The internal uncertainties in the output abundances are due to errors in the atmospheric parameters, atomic data (gf-values) and EW measurements. If we assume that the atmospheric parameters derived above are correct, we can estimate the uncertainty in the final abundances due to the errors between gf-values and in the EW measurements:

$$\sigma_{rand}^2 = \langle \sigma(\log \epsilon(X)) \rangle_{all\ stars}^2 \quad (1)$$

where $\sigma(\log \epsilon(X))$ is the standard deviation of the mean of the abundance of element X given by the individual lines. Note that we can calculate this value only when we have multiple line measurements in a given star. For Li, where we only use the 6707 Å line, we have adopted the σ_{rand} of Fe I for this element.

We use multiple observations of individual stars to quantify the parameter-based uncertainties of our analysis methods. The procedure is based on the assumption that the parameter-based error can be expressed as a single value, and this value can be calculated from a Monte Carlo-like approach. Under this assumption, the optimal way to determine these errors would be to take a large number of spectra of the same star and analyse each spectra using the same methods. All the internal uncertainties would then be expressed in the variance of the stellar parameters and abundances.

Unfortunately, we do not have a large number of observations of the same star, but we do have 18 stars with two or more spectra (41 spectra total). These were used to estimate the internal uncertainties. For each star with multiple observations, the variance between measurements for each abundance was calculated by:

$$\sigma_{mult}^2 = \frac{\sum_{i=1}^N M_i \left(\sum_{j=1}^{M_i} \frac{\sqrt{(\bar{x}_i - x_j)^2}}{M_i} \right)^2}{\sum_{i=1}^N M_i} \quad (2)$$

where N is the 18 stars, each with M observations. The value \bar{x}_i is the mean value of the abundance over the M observations of star i . Note that we use this equation for both the abundances (e.g. [X/H]) and the abundance ratios (e.g. [X/Fe]). We also use Equation 2 to calculate the internal uncertainty of the stellar parameters. We find: $\sigma(T_{eff}) = 40$ K, $\sigma(\log g) = 0.06$, $\sigma([Fe/H]_{atm}) = 0.04$ and $\sigma(\xi) = 0.11$ km/s.

If we assume the errors σ_{rand} and σ_{mult} are independent (in the case of the Fe lines, this is technically not true, as errors in the measurement of these lines can affect the choice of stellar parameters, but we assume that the effect is small), then we get the total internal error by adding in quadrature. Table 7 lists these total errors as $\sigma([X/H])$ and $\sigma([X/Fe])$.

5.2. Effects of Systematic Errors

As revealed in section 4.2, the stellar parameters derived here show some systematic differences from the values derived by others. These differences are probably inevitable, so it is important to understand the effects of potential systematic errors in the parameters on the final derived abundances. As with the internal errors, knowing the potential amplitude of the systematic errors places limits on the conclusions that can be derived from the results.

To understand how systematic errors affect the derived abundance ratios, a series of tests were conducted on a set of 13 stars. These test stars were selected to cover a wide range of temperatures,

evolutionary states, and metallicities. For each test star, the same set of line measurements used in the abundance determinations were run through 10 different atmospheres, each with one or more parameters varied from the original values. The first 8 were cases where only one parameter was varied: $T_{eff} \pm 150$ K, $\log g \pm 0.2$ dex, $[Fe/H]_{atm} \pm 0.3$ dex, and $\xi \pm 0.3$ km/s. In the final two tests, the value of T_{eff} was raised or lowered 150 K and the other parameters were adjusted (following the method described in section 4.1) to make the best fit possible given the new T_{eff} . The mean net effect of the ± 150 K T_{eff} change on the other parameters were: $\log g \pm 0.3$ dex, $[Fe/H]_{atm} \pm 0.1$ dex, and $\xi \pm 0.07$ km/s. The change in ξ varied widely from star to star, while the changes in the other two parameters were more or less the same star-to-star.

For each star in a given test, the resulting abundances for each species were compared to the abundances derived with the original parameters. These differences were averaged over all 13 stars. The results are listed in Table 8. The columns labelled ‘All Vary’ refer to the tests in which the T_{eff} was varied by ± 150 K and the other parameters were allowed to vary as well.

In section 4.1, we noted that the Kurucz atmospheres assume solar ratios for the metals, which does not accurately represent the abundance distribution of metal-poor stars. To account for this, we adjusted the value of $[Fe/H]_{atm}$ upwards in order to increase the free electron supply. As can be seen from Table 8, the net effect on the abundance ratios due to this change is fairly small. The individual star with the largest changes due to adjusting $[Fe/H]_{atm}$ was HIP 57939 (= HD 103095). This star is moderately metal-poor ($[Fe/H] \sim -1.5$) and relatively cool ($T_{eff} = 4950$ K) subdwarf. The abundance ratio changes seen in this star were generally less than twice the listed values. Note that one slightly sensitive species is Fe II, although the net effect would only require an adjustment in $\log g$ of $\lesssim 0.1$ dex to restore the ionization equilibrium.

6. Non-LTE Effects

Allende Prieto *et al.* (1999) compared $\log g$ values for nearby stars derived via Hipparcos parallaxes to literature values obtained via spectroscopic analysis. Their procedure for calculating $\log g$ was similar to what was used section 4.1, although the authors estimated the masses of the stars in their sample by their position on the CMD. They find that for very metal-poor stars ($[Fe/H] < -2.0$) the value of the spectroscopic $\log g$ was significantly lower than the value obtained from the parallax. The authors conclude that the assumption of LTE may not hold for these stars, as an ionizing UV photon can travel much farther in the stellar atmosphere, leading over-ionization compared to LTE conditions.

In Figure 7(a) we plot the difference between the $\log g$ values from this work and Allende Prieto *et al.* (1999) against $[Fe/H]$. There are 3 metal-poor stars which have spectroscopic $\log g$ values significantly lower than their trigometric $\log g$ values. To explore this further, in Figure 7(b) we plot the same quantities, except we expand the sample by using the Hipparcos-based $\log g$ values calculated in this study (the “ $\log g$ init.” column in Table 5). We exclude all stars that are suspected of binarity, have large values of the Hipparcos “goodness of fit” parameter, have $\pi < 10$ mas, or have trigometric $\sigma_{\log g} > 0.2$ dex (assuming the only source of error was from the measurement of the parallax). The three low stars from Figure 6(b) are eliminated by these criteria (suspected of binarity), but one very metal-poor star (HIP 76976 = HD 140283) is added with a spectroscopic $\log g$ value ~ 0.2 dex lower than the Hipparcos-based $\log g$ values. Overall, the spectroscopic $\log g$ values are differ by $\Delta(\log g) = -0.05 \pm 0.04$ (sdm, $N = 71$).

If the claims of Allende Prieto *et al.* (1999) are correct, the $\log g$ of dwarfs with $[Fe/H] < -2.0$ may

need raising by several tenths of a dex. Overall, this would lead to a systematic decrease of nearly all of the abundance ratios. Inspection of the 5 stars tested in section 5.2 with $[\text{Fe}/\text{H}] < -2.0$ shows the systematic changes in abundances are fairly constant, independent of their temperature or evolutionary status. For example, for these 5 stars (HIP 14594, HIP 40068, HIP 68594, HIP 85855 and HIP 87639) if $\log g$ is increased 0.2 dex, the $[\text{Na}/\text{Fe}]$ ratio changes by -0.09 , -0.12 , -0.07 , -0.08 and -0.10 dex, respectively. These changes are somewhat significant when compared to more metal-rich stars, but the relative change between the metal-poor stars remains small.

Thevenin & Idiart (1999) performed extensive detailed calculations of the effect of departures from LTE in populating the energy levels of the Fe I atom and concluded that non-LTE effects may plague abundances derived from Fe I lines, especially in hotter stars ($T_{\text{eff}} > 6000$ K) and subdwarfs of low metallicity. The increase in $[\text{Fe}/\text{H}]$ over LTE determinations was as large as 0.3 dex. They also concluded that Fe abundances derived from Fe II lines, arising generally in atmospheric layers much deeper than those responsible for the Fe I lines, were in fact formed in LTE.

This last point is an important criterion in considering the reliability of the abundances derived in this investigation. Our $[\text{Fe}/\text{H}]$ -values are taken as a mean between $\log \epsilon(\text{FeI})$ and $\log \epsilon(\text{FeII})$, where the Fe II value is taken as fundamental, and the Fe I value is brought into agreement with it (within 0.03 dex) as a means of setting $\log g$. The value of T_{eff} is set explicitly by means of the Fe I lines, via the excitation plot (as explained in Section 4). The question then is whether the $[\text{Fe}/\text{H}]$ -values, based as they are on the assumption that T_{eff} can be derived from LTE analysis of the Fe I lines, are reliable, i.e., satisfy these two criteria: (1) the abundance of Fe II should be fairly independent of the exact value of T_{eff} ; (2) the spectroscopic $\log g$ is in close agreement with the trigometric $\log g$ for the choice of T_{eff} derived by the Fe I excitation plot.

We compare first with the T_{eff} , $\log g$ and $[\text{Fe}/\text{H}]$ tabulations quoted by Thevenin & Idiart (1999), based on the catalog of Thevenin (1998). There are 35 stars in common, all dwarfs, with a range in metallicity from -0.4 to -2.5 in $[\text{Fe}/\text{H}]$. The differences, in the sense “present minus Thevenin & Idiart (1999)”, are $\Delta T_{\text{eff}} = +15 \text{ K} \pm 20 \text{ K}$ (sdm), $\Delta \log g = -0.09 \pm 0.04$, and $\Delta[\text{Fe}/\text{H}] = -0.20 \pm 0.015$. Confining attention to the eleven most metal-poor dwarfs does not change the result: $\Delta T_{\text{eff}} = +38 \text{ K} \pm 40 \text{ K}$, $\Delta \log g = -0.06 \pm 0.05$ and $\Delta[\text{Fe}/\text{H}] = -0.19 \pm 0.03$. The Thevenin & Idiart (1999) $\log g$ and $[\text{Fe}/\text{H}]$ values are those “adjusted” for non-LTE effects in Fe I, and the latter turn out to be higher than those based on the conventional LTE results by about 0.2 dex.

Except for $[\text{Fe}/\text{H}]$, the changes are quite small. Thevenin & Idiart (1999) suggest that their values of $\log g$ are close to those expected on the average based on the Hipparcos parallaxes. Our values of $\log g$ are only slightly smaller, as was seen in the comparison to Hipparcos-based $\log g$ values above (Figure 6). The difference is in the same direction and has a value (within the errors) much like that of our difference in $\log g$ compared with Allende Prieto *et al.* (1999).

The above argument assumes that our values of T_{eff} are, of course, accurate. The important point however, in the context of the present study, is the effect of the choice of T_{eff} on the abundance scale. The Fe II abundance is fairly independent of T_{eff} . We see that from inspection of Table 8, where it is seen that the $[\text{Fe II}/\text{H}]$ -abundance scarcely changes over a 300 K change in T_{eff} . The reason for this has to do with the ionization equilibrium of Fe: at optical depths greater than 0.1 in subdwarf atmospheres in the T_{eff} range from 5000–6200 K, the minority of the Fe is in the form of Fe I. In deeper layers and in hotter stars, less than 10 percent of the Fe is in the form of Fe I. Thus, changes of a few hundred degrees in T_{eff} have little effect on $\log \epsilon(\text{FeII})$. Certainly the increase of 38 K necessary to place us on the T_{eff} scale of (say) Alonso *et al.* (1995) would have a negligible effect.

Finally, we note the difference of 0.2 dex between our $[\text{Fe}/\text{H}]$ values and the non-LTE “adjusted” values of Thevenin & Idiart (1999). The Thevenin & Idiart (1999) catalog contains $[\text{Fe}/\text{H}]$ -values that are “means” of determinations from the literature, based on LTE analysis of (mostly) Fe I lines. They are subject, of course, to systematic errors in g -values, EWs, effective temperatures, etc, and we have no way to judge those. What is valuable in Thevenin & Idiart (1999) is not the assumed set of “absolute” LTE $[\text{Fe}/\text{H}]$ values, but rather the corrections to those values based on non-LTE considerations.

7. Summary

We have observed and analyzed elemental abundances for 168 stars (mostly dwarfs) using 191 high-resolution, high-S/N spectra. The methods used to determine the parameters and abundances are self-consistent and should provide accurate relative abundances for the target stars. The overall precision of the abundances ultimately depends on how well the basic assumptions of the analysis hold, which are: 1) the abundances of the elements considered can be determined accurately by plane-parallel atmospheres using an LTE analysis, 2) the T_{eff} of the stars can be determined by the plot of abundance vs excitation potential for Fe I, 3) the surface gravity can be determined by matching iron abundances determined by the neutral and singly ionized lines, 4) the microturbulent velocity can be determined by the abundance vs line strength plot for Fe I, and 5) the van der Waals damping parameter can be accurately determined by the Unsöld (1955) approximation.

To test these assumptions, we have compared the stellar parameters we derive against independent measurements, and we study the effects of parameter variations on the resulting abundances. Our T_{eff} scale is consistent with independent determinations (including the non-LTE scale of Thevenin & Idiart 1999) to within a small offset. Our surface gravities also compare well with Hipparcos-based values, although we lack data for stars with $[\text{Fe}/\text{H}] < -2$, which is where Allende Prieto *et al.* (1999) suggest non-LTE effects exist. More importantly, we show that any reasonable variation in the derived parameters does not cause drastic changes in the derived abundance ratios.

The papers of this series make up the PhD thesis of JPF. JPF is grateful to R. P. Kraft, R. Peterson, M. Bolte, and P. Guhathakura for their insights, advice and efforts on his PhD committee. He also wishes to acknowledge M. Shetrone, J. Johnson, and T. Misch for their thoughtful comments and assistance with observations. Special thanks goes to the anonymous referee who provided several useful comments. This research was supported by NSF Contract AST 96-18351 to RPK.

REFERENCES

- Allende Prieto, C., Garcia Lopez, R. J., Lambert, D. L., & Gustafsson, B. 1999, *ApJ*, 527, 879.
- Alonso, A., Arribas, S., & Martínez-Roger, C. 1995, *A&A*, 297, 179.
- Anders, E. & Grevesse, N. 1989, *Geochim. Cosmochim. Acta*, 53, 197.
- Beers, T. C. & Sommer-Larsen, J. 1995, *ApJS*, 96, 175.
- Beveridge, C. R. & Sneden, C. 1994, *AJ*, 108, 285.
- Bizzarri, A., Huber, M. C. E., Noels, A., Grevesse, N., Bergeson, S. D., Tsekeris, P., & Lawler, J. E. 1993, *A&A*, 273, 707.
- Blackwell, D. E. & Shallis, M. J. 1977, *MNRAS*, 180, 177.
- Blackwell, D. E., Ibbetson, P. A., Petford, A. D., & Shallis, M. J. 1979a, *MNRAS*, 186, 633.
- Blackwell, D. E., Petford, A. D., & Shallis, M. J. 1979b, *MNRAS*, 186, 657.
- Blackwell, D. E., Petford, A. D., Shallis, M. J., & Simmons, G. J. 1980a, *MNRAS*, 191, 445.
- Blackwell, D. E., Petford, A. D., Shallis, M. J., & Simmons, G. J. 1980b, *A&A*, 81, 340.
- Blackwell, D. E., Petford, A. D., Shallis, M. J., & Leggett, S. 1982a, *MNRAS*, 199, 21.
- Blackwell, D. E., Petford, A. D., Shallis, M. J., & Simmons, G. J. 1982b, *MNRAS*, 199, 43.
- Blackwell, D. E., Petford, A. D., & Simmons, G. J. 1982c, *MNRAS*, 201, 595.
- Blackwell, D. E., Menon, S. L. R., & Petford, A. D. 1984, *MNRAS*, 207, 533.
- Blackwell, D. E., Booth, A. J., Menon, S. L. R., & Petford, A. D. 1986, *MNRAS*, 220, 289.
- Bond, H. E. 1980, *ApJS*, 44, 517.
- Carney, B. W. 1983, *AJ*, 88, 623.
- Carney, B. W., Latham, D. W., Laird, J. B. & Aguilar, L. A. 1994, *AJ*, 107, 2240.
- Carney, B. W., Wright, J. S., Sneden, C., Laird, J. B., Aguilar, L. A. & Latham, D. W. 1997, *AJ*, 114, 363.
- Cavallo, R. M., Pilachowski, C. A. & Rebolo, R. *PASP*, 109, 226.
- Cayrel de Stobel, G., Soubiran, C., Friel, E. D., Ralite, N. & Francois, P. 1997, *A&AS*, 124, 299.
- Edvardsson, B., Andersen, J., Gustafsson, B., Lambert, D. L., Nissen, P. E. & Tomkin, J. 1993, *A&A*, 275, 101.
- ESA 1997, The *Hipparcos* and *Tycho* Catalogues (ESA SP-1200) (Noordwijk: ESA).

- Fuhr, J. R., Martin, G. A., & Wiese, W. L. 1988, *J. Phys. Chem. Ref. Data*, 17, No. 4.
- Fuhrmann, K., Axer, M., & Gehren, T. 1995, *A&A*, 301, 492.
- Fulbright, J. P. & Kraft, R. P. 1999, *AJ*, 118, 527.
- Garz, T. 1973, *A&A*, 26, 471.
- Gratton, R. G. & Sneden C. 1987, *A&A*, 178, 179.
- Gratton, R. G. & Sneden C. 1988, *A&A*, 204, 193.
- Gratton, R. G. & Sneden C. 1990, *A&AS*, 86, 269.
- Gratton, R. G. & Sneden C. 1991, *A&A*, 241, 501.
- Gratton, R. G. & Sneden C. 1994, *A&A*, 287, 927.
- Gratton, R. G., Carretta, E. & Castelli, F. 1996, *A&A*, 314, 191.
- Gray, D. F. 1992, *The Observation and Analysis of Stellar Atmospheres* (2nd ed.; Cambridge: Cambridge University Press).
- Hanson, R. B., Sneden, C., Kraft, R. P. & Fulbright, J. P. 1998, *AJ*, 116, 1286.
- Ivans, I. I., Sneden, C., Kraft, R. P., Suntzeff, N. B., Smith, V. V., Langer, G. E. & Fulbright, J. P. 1999, *AJ*, 118, 1273.
- King, J. R. 1997, *AJ*, 113, 2302.
- Johnson, J. A. 1999, Ph.D. thesis, University of California-Santa Cruz.
- McWilliam, A., Preston, G. W., Sneden, C., & Searle, L. 1995b, *AJ*, 109, 2757.
- McWilliam, A. 1997, *ARA&A*, 35, 503.
- McWilliam, A. 1998, *AJ*, 115, 1640.
- Moity, J. 1983, *A&AS*, 52, 37.
- Moore, C. E., Minnaert, M. G. J., & Houtgast, J. 1966, *The Solar Spectrum 2935 Å to 8770 Å* (NBS Monograph 61) (Washington: NBS).
- Nissen, P. E. & Schuster, W. J. 1997, *A&A*, 326, 751.
- O'Brian, T. R., Wickliffe, M. E., Lawler, J. E., Whaling, W., & Brault, J. W. 1991, *J. Opt. Soc. Am. B*, 8, 1185.
- Olsen, E. H. 1994, *A&AS*, 106, 254.
- Pilachowski, C. A., Sneden, C. & Booth, J. 1993, *ApJ*, 407, 699.

- Ryan, S. G., Norris, J. E., & Bessel, M. S. 1991, AJ, 102, 303.
- Sandage, A. & Fouts, G. 1987, AJ, 93, 74.
- Schuster, W. J. & Nissen, P. E. 1988, A&AS, 73, 225.
- Schuster, W. J. & Nissen, P. E. 1989, A&A, 221, 65.
- Schuster, W. J., Parrao, L. & Cantreiras Martinez, M. E. 1993, A&AS, 97, 951.
- Shetrone, M. D. 1996, AJ, 112, 1517.
- Smith, G. & Raggett, D. St. J. 1981, J. Phys. B, 14, 4015.
- Smith, V. V., Lambert, D. L. & Nissen, P. E. 1998, ApJ, 506, 405.
- Snedden, C. 1973, ApJ, 184, 839.
- Snedden, C., McWilliam, A., Preston, G. W., Cowan, J. J., Burris, D. L., & Armosky, B. J. 1996, ApJ, 467, 819.
- Snedden, C., Kraft, R. P., Shetrone, M. D., Smith, G. H., Langer, G. E., & Prosser, C. F. 1997, AJ, 114, 1964.
- Stephens, A. 1999, AJ, 117, 1771.
- Thevenin, F. & Idiart, T. P. 1999, ApJ, 521, 753.
- Thevenin, F. 1998, Chemical Abundances in Late-Type Stars, CDS Information Bull. 49, in press
- Tinsley, B. M. 1979, ApJ, 229, 1046.
- Unsöld, A. 1955, Physik der Sternatmosphären (2nd ed.; Berlin: Springer-Verlag).
- Vogt, S. S. 1987, PASP, 99, 1214.
- Vogt, S. S., Allen, S. L., Bigelow, B. C., Bresee, L., Brown, B., Cantrall, T., Conrad, A., Couture, M., Delaney, C., Epps, H. W., Hilyard, D., Hilyard, D. F., Horn, E., Jern, N., Kanto, D., Keane, M. J., Kibrick, R. I., Lewis, J. W., Osborne, J., Pardeilhan, G. H., Pfister, T., Ricketts, T., Robinson, L. B., Stover, R. J., Tucker, D., Ward, J. & Wei, M. Z. 1994, SPIE, 2198, 362.
- Wheeler, J. C., Snedden, C. & Truran Jr., J. W. 1989, ARA&A, 27, 279.
- Wickliffe, M. E. & Lawler, J. E. 1997, ApJS, 110, 163.

Fig. 1.— Comparison of the equivalent width (EW) measurements between the Sandiford spectrograph (McDonald 2.1-m) and Hamilton spectrograph (Lick 3-m and CAT).

Fig. 2.— Comparisons of equivalent width (EW) measurements from this paper and (a) Edvardsson *et al.* (1993), (b) Gratton & Sneden (1990), (c) Nissen & Schuster (1997) and (d) Johnson (1999).

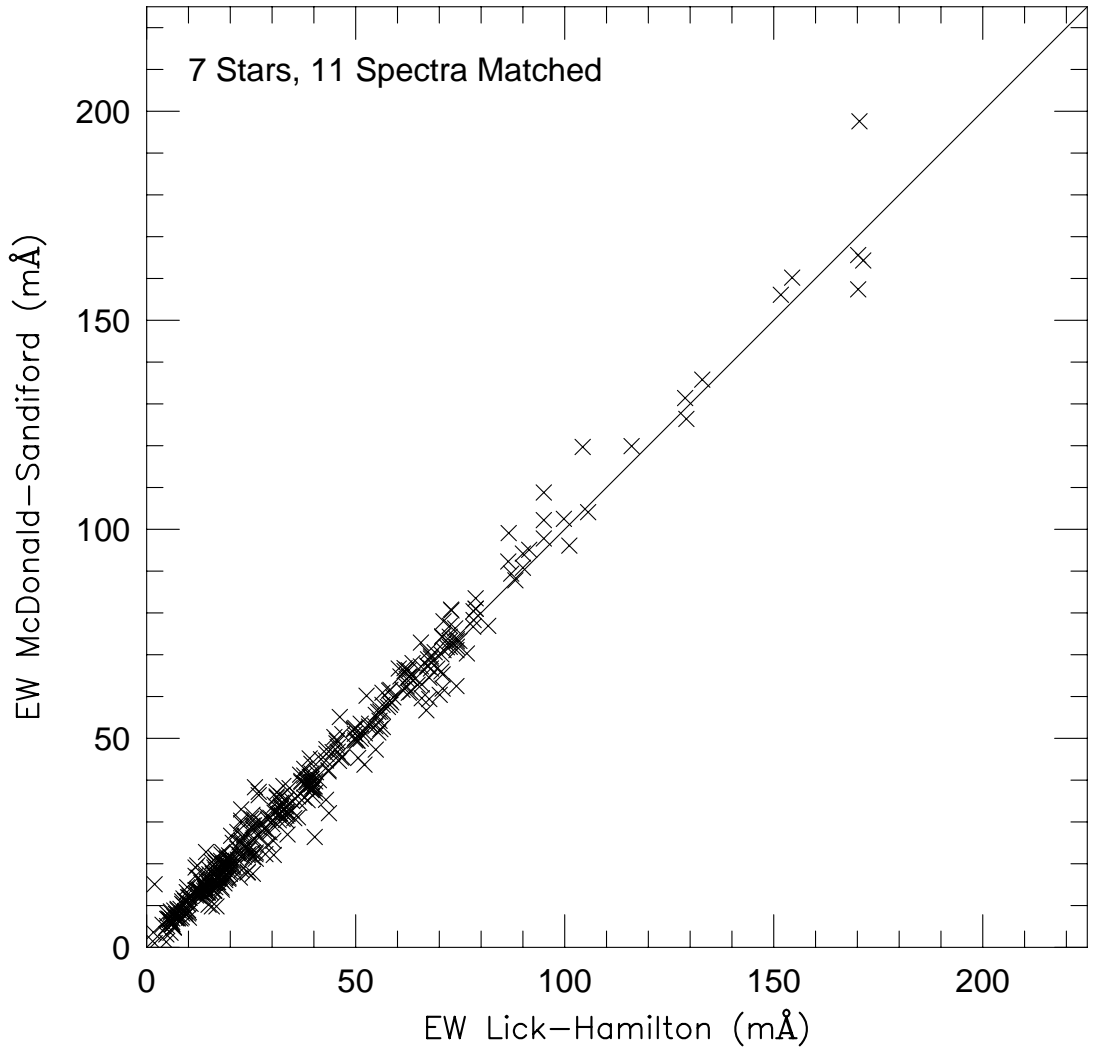
Fig. 3.— T_{eff} value comparisons between this work and (a) Alonso *et al.* (1995), (b) Carney *et al.* (1994), (c) Carney (1983) and (d) various literature studies.

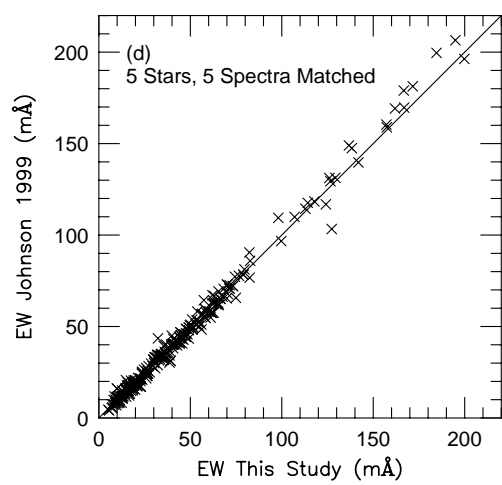
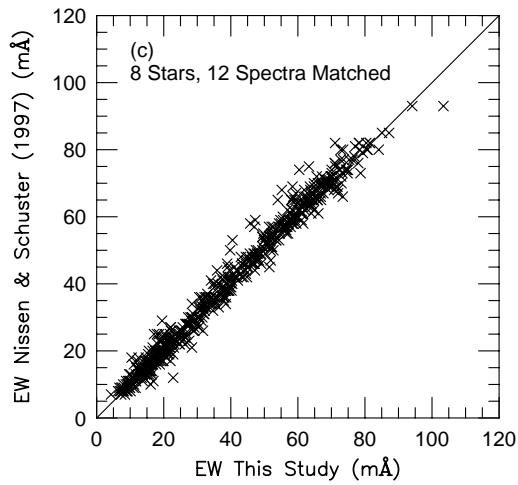
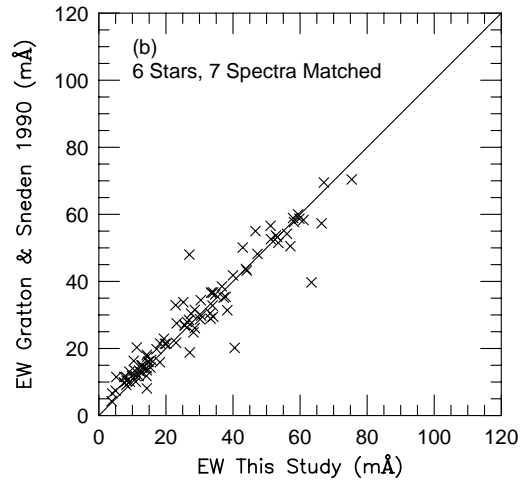
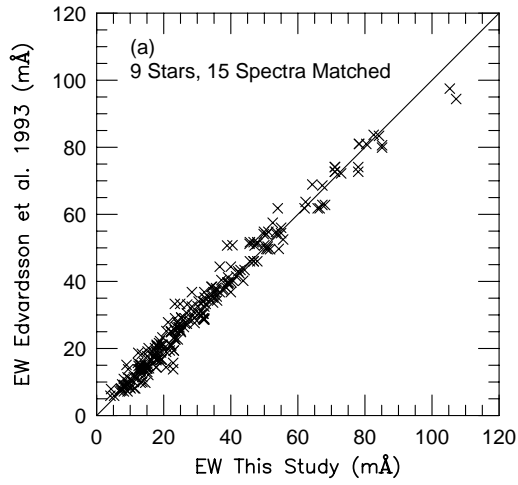
Fig. 4.— (a) T_{eff} and (b) $\log g$ value comparisons between this work and Gratton *et al.* (1996). The structure seen at low temperatures and surface gravities (also seen in Figure 3(c) seem to be due to differences between the photometric and spectroscopic T_{eff} scales for giant stars.

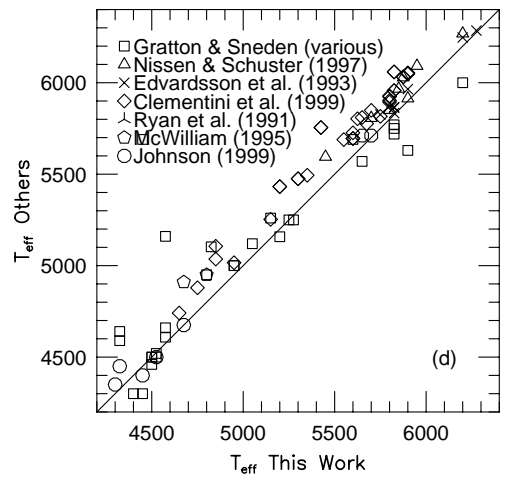
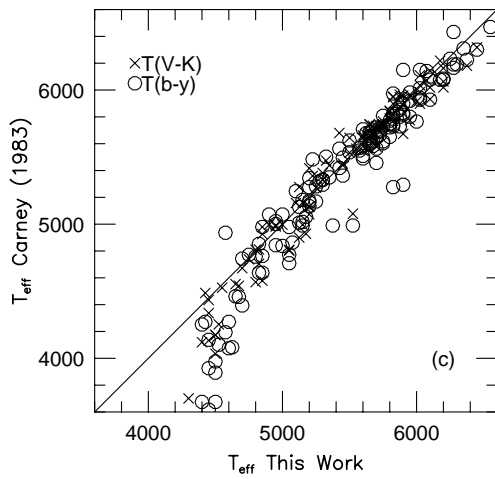
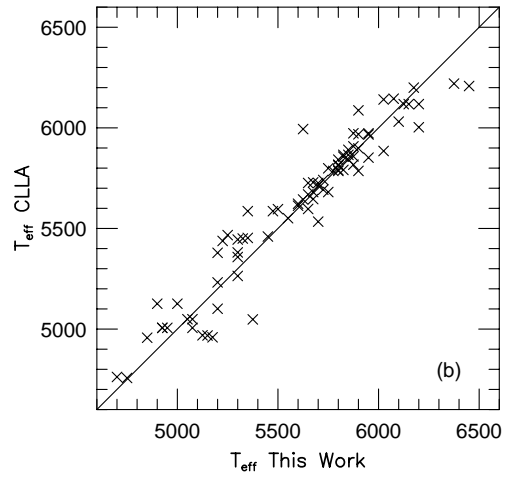
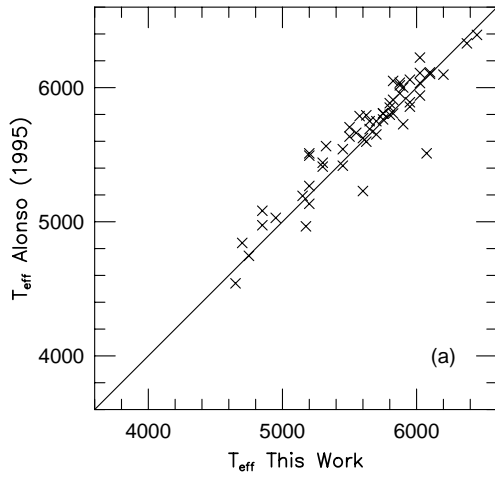
Fig. 5.— Comparison of the value of $[\text{Fe}/\text{H}]$ derived by the Carney *et al.* (1994) survey and this work.

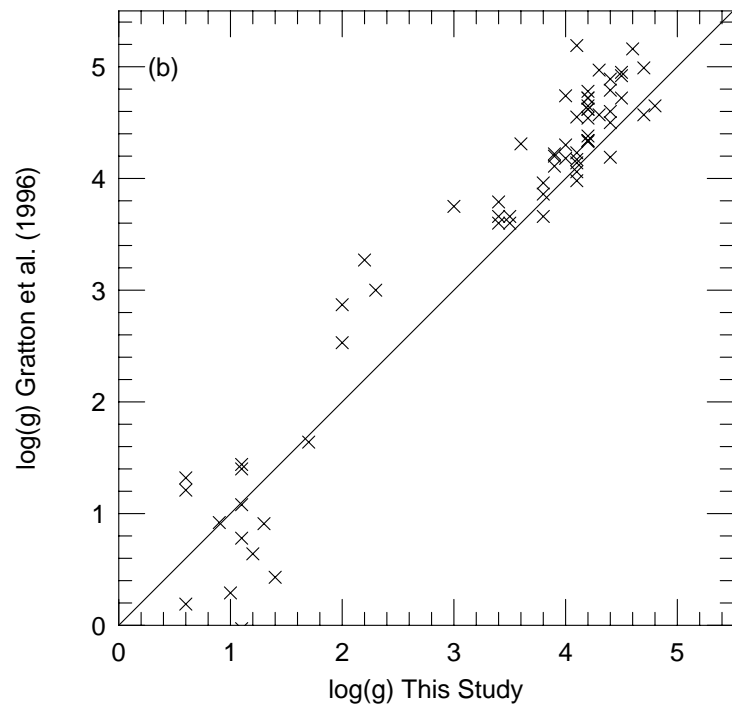
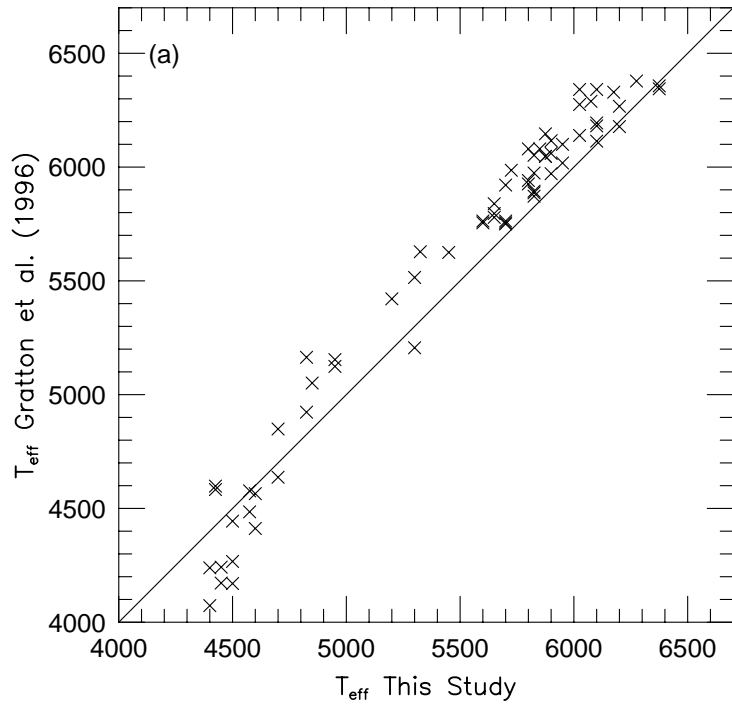
Fig. 6.— Histograms of the various stellar parameters. (a) and (b) show that the most common star in the survey is a solar-like metal-deficient dwarf, although there a number of subgiants and giants included in the survey as well.

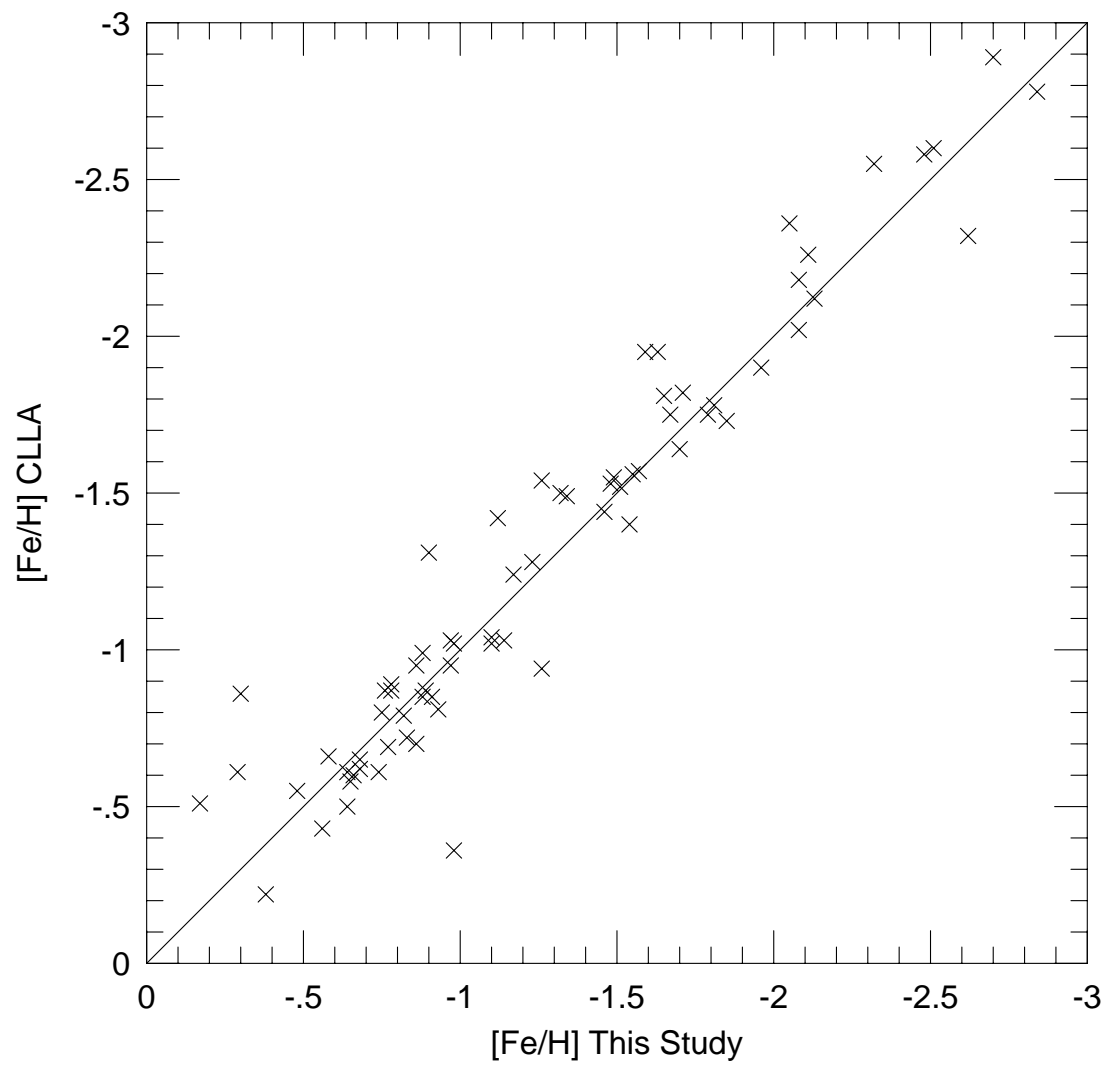
Fig. 7.— Comparisons between the value of $\log g$ derived spectroscopically in this work against the value derived from Hipparcos parallax distances (the ‘trigometric’ $\log g$). Panel (a) compares against the values determines by Allende Prieto *et al.* (1999), while panel (b) compares the spectroscopic result of this work against the initial trigometric estimate, for those stars listed in Table 6 with reliable parallax values.

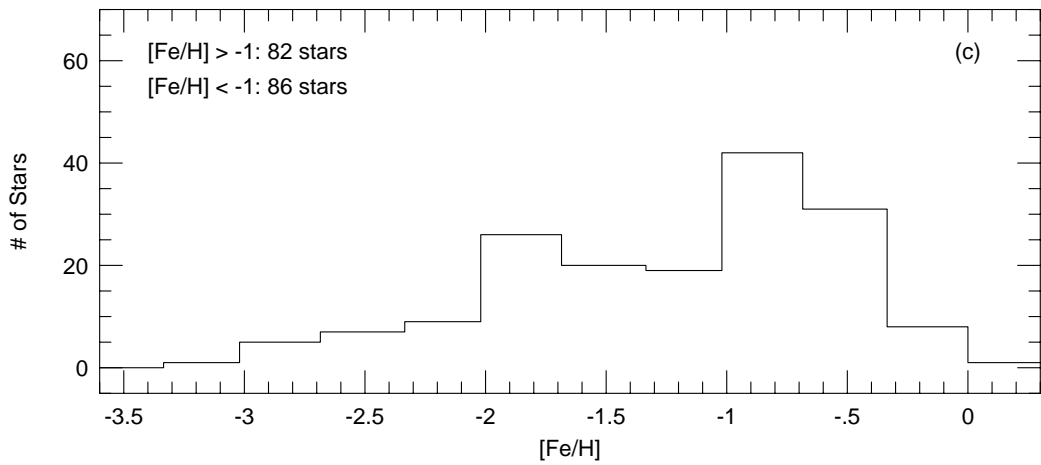
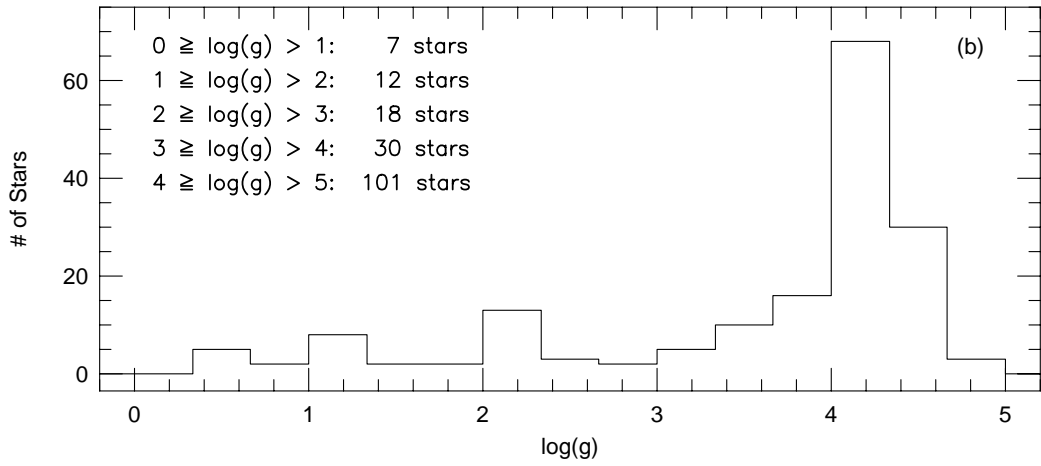
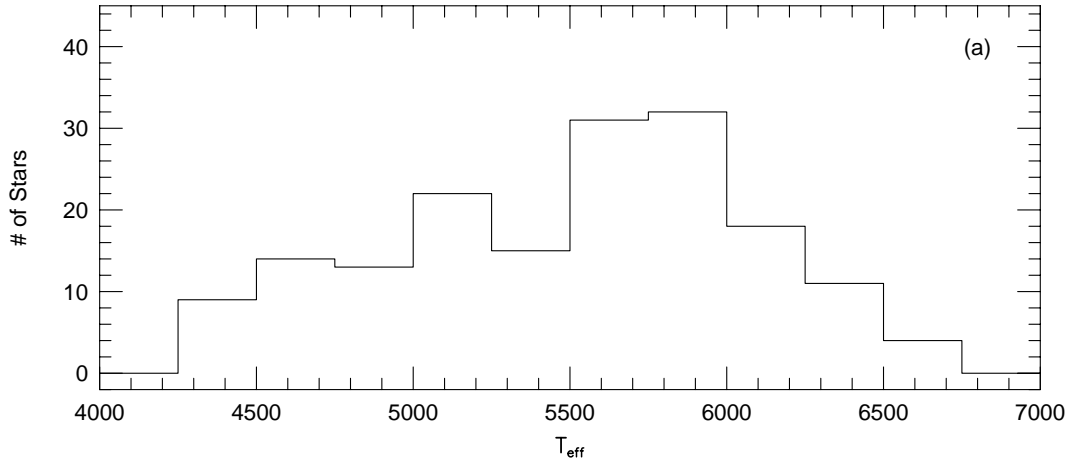












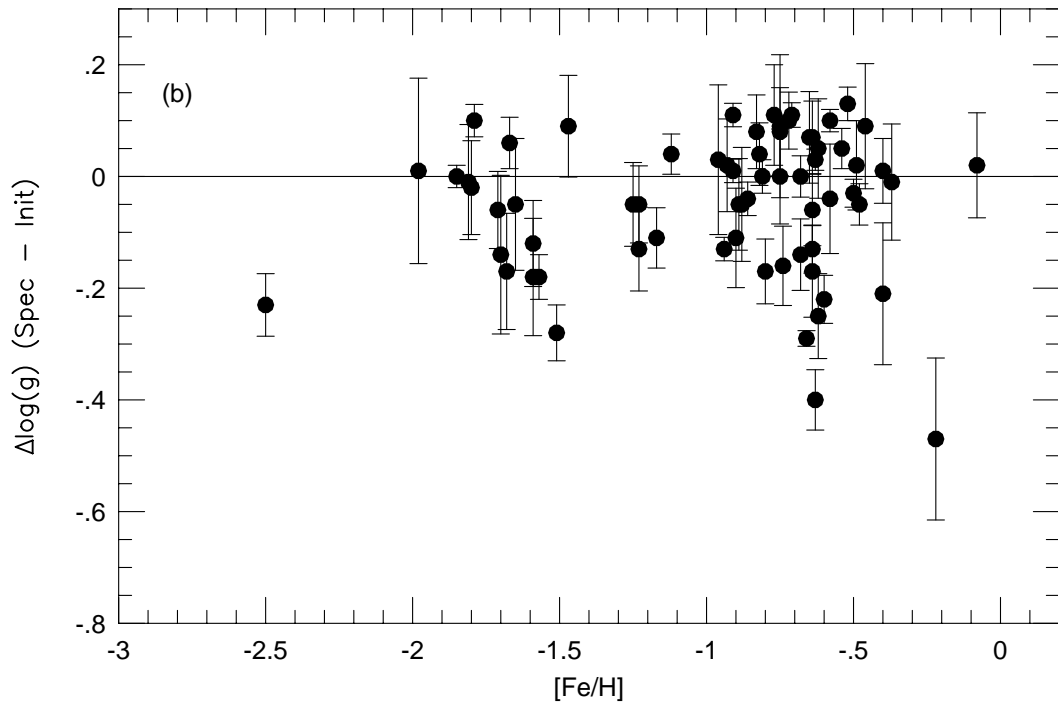
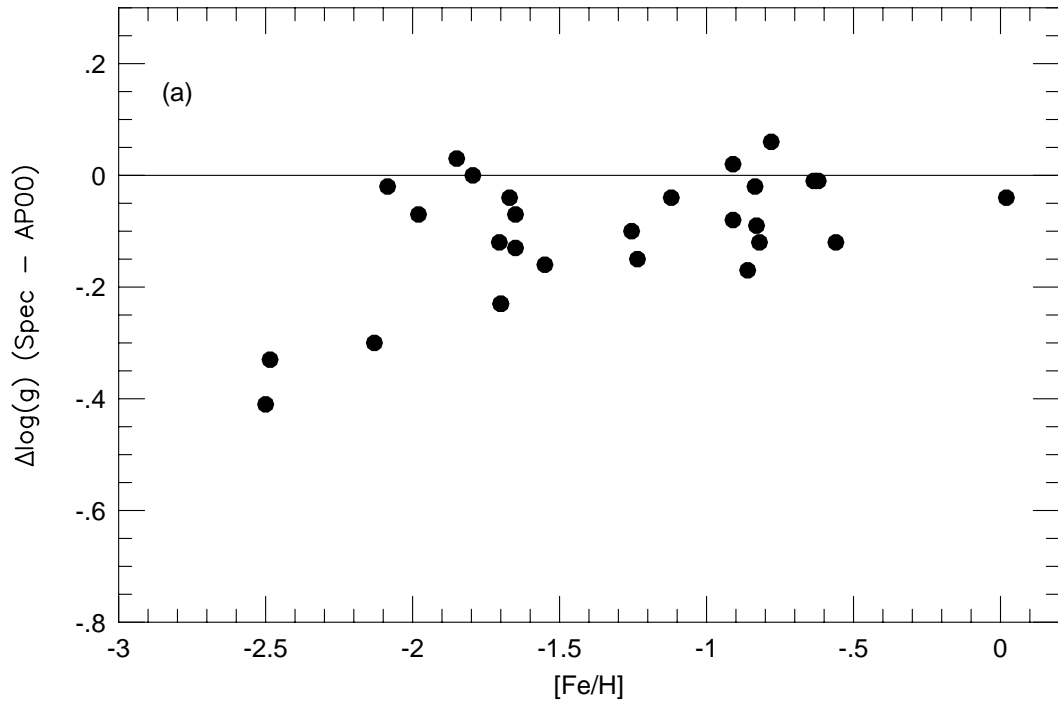


TABLE 1. Log of Observing Runs

Run	Dates	Telescope	Instrument	$\lambda\lambda$ Coverage (approx.)
Sep94	18 September 1994	Lick 3-m	Hamilton	4460–7090 Å (incomplete)
Nov94	12 November 1994	Lick 3-m	Hamilton	4460–7090 Å (incomplete)
Jun95	10 June 1995	Lick 3-m	Hamilton	3900–10075 Å
Oct97	18–20 October 1997	Lick 0.6-m CAT	Hamilton	3650–10750 Å
ESO	24 November 1997	ESO 3.6-m	CASPEC	5700–8160 Å (incomplete)
Mar98	17–18 March 1998	Lick 3-m	Hamilton	3700–10075 Å
K98	26 March 1999	Keck I 10-m	HIRES	4380–6780 Å (incomplete)
Jun98	7–8 June 1998	Lick 3-m	Hamilton	3700–10075 Å
Jul98	28 July 1998	Lick 3-m	Hamilton	3800–8850 Å
Aug98	8–9 August 1998	Lick 3-m	Hamilton	4140–9900 Å
A98	10–11 August 1998	Lick 3-m	Hamilton	3800–8850 Å
Oct98	30–31 October 1998	Lick 3-m	Hamilton	4140–9900 Å
Jan99	26–31 January 1999	McDonald 2.1-m	Sandiford	5300–6500 Å
K99	23 March 1999	Keck I 10-m	HIRES	3760–6180 Å (incomplete)
Apr99	6–7 April 1999	Lick 3-m	Hamilton	4140–9900 Å
May99	24 May 1999	Lick 3-m	Hamilton	4140–9900 Å

TABLE 2. Table of Observations^a

HIP	Observ. Run	HD	BD/CD	Other	V	Exp. (s)	S/N
SUN	Oct98	-26.75	1	80
SUN	May99	-26.75	45	220
171	Oct98	224930	BD +26 4734	GL914A	5.80	300	200
2413	Oct98	2665	BD +56 70	...	7.72	2000	105
3026	Aug98	3567	BD -09 122	G270-23	9.25	1800	120
3086	Jul98	3628	BD +2 84	G1-9	7.34	900	110
3554	Aug98	4306	BD -10 155	...	9.02	1500	110
5336	Aug98	6582	BD +54 223	G34-3	5.17	300	250
5445	Aug98	6755	BD +60 170	...	7.72	900	160
5458	Oct98	6833	BD +53 236	...	6.75	900	70
6710	Oct98	8724	BD +16 149	...	8.30	900	75
7217	Aug98	9430	BD +22 245	G34-36	9.04	1500	115
10140	Sep94	...	BD +29 366	G74-5	8.76	2700	115
10140	Aug98	...	BD +29 366	G74-5	8.76	1200	120
10449	Oct98	...	BD -01 306	G159-50	9.08	1800	100
11349	Aug98	15096	BD +05 336	G73-57	7.93	900	140
11952	Oct98	16031	BD -13 482	...	9.77	3600	90
12306	Oct97	16397	BD +30 421	G36-38	7.34	8100	205
13366	A98	17820	BD +10 380	G4-44	8.38	900	90
14086	Oct98	18907	CD -28 987	LTT1446	5.88	300	110
14594	Nov94	19445	BD +25 495	G37-26	8.04	2700	145
14594	Oct98	19445	BD +25 495	G37-26	8.04	900	130
15394	Oct97	20512	BD +14 550	G5-27	7.41	5400	125
16214	Oct98	21581	BD -00 552	...	8.70	1200	90
17085	ESO	22785	BD -04 641	...	9.58	1200	135
17147	Nov94	22879	BD -03 592	G80-15	6.68	1200	145
17147	Oct98	22879	BD -03 592	G80-15	6.68	600	155
17147	Jan99	22879	BD -03 592	G80-15	6.68	1200	100
17666	Oct98	23439	BD +41 750	G95-57	7.67	900	135
17666	Jan99	23439	BD +41 750	G95-57	7.67	1800	75
18235	Oct98	24616	CD -23 1619	LTT1823	6.68	900	100
18915	Oct98	25329	BD +34 796	...	8.51	1500	140
18995	Oct98	25532	BD +22 626	...	8.22	1200	110
19007	ESO	25673	BD -05 812	...	9.53	1200	165
19378	Oct98	26297	BD -16 791	...	7.46	1200	110
19797	Nov94	284248	BD +21 607	G8-16	9.23	2400	85
19797	Oct98	284248	BD +21 607	G8-16	9.23	1800	90
21000	K98	...	BD +4 701	...	9.83	360	90
21586	K98	...	BD +50 1021	G175-43	10.39	360	95
21609	ESO	29907	CD -65 253	LTT2057	9.91	2400	200
21648	Jan99	29574	BD -13 942	...	8.33	1850	65
21767	K98	280067	BD +34 899	...	10.40	360	100
22246	K98	...	BD +45 983	G96-1	10.12	400	90
22632	ESO	31128	CD -27 1935	LTT2108	9.13	900	170
23344	Oct98	...	BD +03 740	G84-29	9.79	3600	100
24316	ESO	34328	CD -59 1024	LTT2211	9.46	1200	170
26688	ESO	37792	BD -19 1234	...	7.70	300	200
27654	Jan99	39364	BD -20 1211	delLep	3.76	180	230
28188	K98	40057	BD +21 1056	...	9.00	180	115
29759	Oct98	...	BD +37 1458	G98-58	8.92	3600	160
29992	Jan99	44007	BD -14 1399	...	8.05	1800	100
30668	Jan99	45282	BD +03 1247	...	8.00	1800	135
30990	Jan99	45205	BD +60 970	G249-49	8.43	2400	105
31188	Jan99	46341	BD -06 1598	...	8.60	4915	100
31639	K98	...	CD -25 3416	...	9.64	720	115
32308	K98	...	BD +15 1305	...	10.73	450	145
33582	Jan99	51754	BD -00 1520	G108-43	9.02	2700	65
34146	ESO	53545	BD -16 1743	...	8.05	360	175
34548	Mar98	53871	BD +52 1173	...	9.06	2000	155
36491	Mar98	59374	BD +19 1749	G88-31	8.48	1200	175
36849	Jan99	60319	LTT12040	G88-40	8.94	2700	130
37335	Nov94	...	BD -01 1792	G112-36	9.23	3600	95
38541	Mar98	64090	BD +31 1684	G90-25	8.27	1200	190
38621	Jan99	63791	BD +62 959	...	7.89	1200	125
38625	Oct97	64606	BD -01 1883	G112-54	7.44	5400	125
40068	K99	...	BD +80 245	G251-54	10.01	600	145
40778	K98	233511	BD +54 1216	G194-22	9.73	600	150
42592	Jan99	74000	BD -15 2546	...	9.67	3600	105
44075	Jan99	76932	BD -15 2656	...	5.80	600	220
44116	Mar98	76910	BD -00 2103	...	8.48	1200	190
44124	Nov94	...	BD -03 2525	G114-26	9.66	4800	75
44716	Jan99	78050	BD +21 1969	G9-47	7.68	1200	140
44919	Jan99	78737	CD -26 6774	...	8.92	1260	50
47139	Jan99	83212	BD -20 2955	...	8.33	1800	125
47640	Mar98	83888	BD +46 1535	...	8.84	1200	150
48146	Mar98	...	BD +09 2242	...	9.57	2400	140
48152	Mar98	84937	BD +14 2151	G43-3	8.33	1200	180
49371	Jan99	87140	BD +55 1362	...	8.97	3600	140
50139	Jun95	88725	BD +03 2338	G44-6	7.75	240	85
50173	Jan99	88609	BD +54 1359	...	8.59	1800	100
52771	Jan99	...	BD +29 2091	G119-32	10.26	3600	45
53070	Jun95	94028	BD +21 2247	G58-25	8.21	500	110

TABLE 2. (continued)

HIP	Observ. Run	HD	BD/CD	Other	V	Exp. (s)	S/N
54858	Jan99	97560	BD +40 2408	G122-6	7.91	1200	140
55022	Jan99	97916	BD +02 2406	...	9.21	3600	70
57265	K99	...	BD +26 2251	G121-12	10.38	600	135
57850	Jan99	103036	BD -04 3155	...	8.19	1200	110
57850	Apr99	103036	BD -04 3155	...	8.19	1800	65
57939	Jun95	103095	BD +38 2285	G122-51	6.42	300	210
57939	Mar98	103095	BD +38 2285	G122-51	6.42	300	240
57939	Jun98	103095	BD +38 2285	G122-51	6.42	60	70
57939	Jan99	103095	BD +38 2285	G122-51	6.42	3600	130
58229	K99	103723	BD -20 3540	...	10.06	600	145
58357	Jan99	103912	BD +49 2098	G122-57	8.35	3600	140
59109	K99	...	BD -04 3208	G13-9	10.00	600	160
59239	Jan99	105546	BD +59 1422	...	8.61	2700	70
59330	Jan99	105755	BD +55 1514	...	8.58	2700	60
59750	Mar98	106516	BD -09 3468	...	6.11	300	220
59750	Jan99	106516	BD -09 3468	...	6.11	600	125
59750	Apr99	106516	BD -09 3468	...	6.11	600	85
60551	Jan99	108076	BD +39 2519	G123-29	8.03	1200	105
60632	Mar98	108177	BD +02 2538	G13-35	9.66	2400	120
60719	Jan99	108317	BD +06 2613	...	8.03	1200	65
60719	Apr99	108317	BD +06 2613	...	8.03	1800	60
61824	Jan99	110184	BD +09 2653	...	8.27	1200	75
61824	Apr99	110184	BD +09 2653	...	8.27	1800	50
62747	Jun98	111721	BD -12 3709	...	7.99	1200	130
62882	Mar98	111980	BD -17 3723	...	8.36	1200	155
63970	Mar98	...	BD +33 2300	...	10.07	3600	155
64115	May99	114095	BD -06 3742	G14-32	8.35	900	105
64426	May99	114762	BD +18 2700	G63-9	7.30	600	145
65268	Mar98	116316	BD +26 2452	...	7.64	900	230
66246	May99	118055	BD -15 3695	...	8.86	1500	100
66509	Jun95	118659	BD +19 2692	G63-44	7.97	1000	125
66665	Jun98	...	BD +13 2698	G63-46	9.37	1200	70
66815	Mar98	119173	BD -03 3515	...	8.83	1200	140
68594	Jun98	122563	BD +10 2617	...	6.18	120	95
68796	Mar98	123710	BD +75 526	...	8.21	1200	170
68807	May99	122956	BD -14 3867	...	7.22	600	125
69746	May99	...	BD +09 2870	...	9.40	1800	85
70647	May99	126587	BD -21 3903	...	9.11	1800	65
70681	Jun98	126681	BD -17 4092	...	9.28	1500	55
71886	Mar98	129392	BD +04 2902	...	8.94	1500	115
71887	Mar98	129515	BD +32 2505	...	8.79	1800	165
71939	Mar98	129518	BD +04 2904	...	8.81	1800	170
72461	Mar98	...	BD +26 2606	G166-45	9.73	2400	145
73385	Jun98	132475	BD -21 4009	...	8.55	900	75
73960	May99	...	BD +30 2611	...	9.13	1800	120
74033	Jun98	134113	BD +09 3001	G66-65	8.26	720	100
74067	Aug98	134088	BD -07 3963	G151-28	7.99	900	125
74079	Jun98	134169	BD +04 2969	...	7.67	360	80
74234	Jun95	134440	BD -15 4041	GL579.2B	9.44	2000	110
74235	Jun95	134439	BD -15 4042	GL579.2A	9.07	2000	130
76976	Jun95	140283	BD -10 4149	GJ1195	7.20	450	135
76976	Mar98	140283	BD -10 4149	GJ1195	7.20	600	200
77946	Jun98	142575	BD +05 3113	...	8.61	900	80
78640	Jun98	...	BD +42 2667	G180-24	9.86	2700	85
80837	Jun95	148816	BD +04 3195	G17-21	7.27	800	180
81170	Jun95	149414	BD -03 3968	G17-25	9.60	2000	105
81461	Aug98	149996	BD -02 4219	G17-30	8.50	900	100
85007	Sep94	157466	BD +25 3252	...	6.88	800	195
85007	Jun95	157466	BD +25 3252	...	6.88	600	180
85007	Jun98	157466	BD +25 3252	...	6.88	180	85
85378	Jun95	158226	BD +31 3027	G181-47	8.50	2000	200
85757	Sep94	158809	BD -02 4381	G19-27	8.15	2700	165
85855	Jun98	...	BD +23 3130	G170-47	8.94	1200	80
85855	Aug98	...	BD +23 3130	G170-47	8.94	3600	175
86013	Aug98	159482	BD +06 3455	G139-48	8.37	900	110
86431	Jun98	160693	BD +37 2926	G182-19	8.39	720	90
86443	K99	...	BD +02 3375	G20-8	9.94	450	145
87693	Aug98	...	BD +20 3603	G183-11	9.77	2700	105
88010	Aug98	163810	BD -13 4807	G154-36	9.63	2700	95
88039	May99	163799	BD -22 4475	...	8.80	1500	85
91058	Jun95	171620	BD +34 3239	...	7.55	1200	250
92167	May99	175305	BD +74 792	G259-35	7.18	600	105
92532	Sep94	174912	BD +38 3327	G207-5	7.15	900	175
92532	Jun95	174912	BD +38 3327	G207-5	7.15	700	220
92781	Jun98	175179	BD -04 4617	...	9.05	1200	55
94449	Aug98	179626	BD -00 3676	G22-20	9.18	1800	120
96115	Aug98	338529	BD +26 3578	...	9.37	1800	110
96185	Oct97	184499	BD +32 3474	...	6.62	3600	200
96185	Aug98	184499	BD +32 3474	...	6.62	450	200
97023	Aug98	186379	BD +24 3849	...	6.87	450	160
97468	Oct98	187111	BD -12 5540	...	7.71	900	55
98020	Jun98	188510	BD +10 4091	G143-17	8.83	1200	60

TABLE 2. (continued)

HIP	Observ. Run	HD	BD/CD	Other	V	Exp. (s)	S/N
98532	Jul98	189558	BD -12 5613	...	7.72	900	85
99423	Aug98	345957	BD +23 3912	...	8.90	1200	110
99938	Aug98	192718	BD -07 5253	...	8.39	900	115
100568	Aug98	193901	BD -21 5703	...	8.65	1200	100
100792	Aug98	194598	BD +09 4529	G24-15	8.33	900	120
101346	Aug98	195633	BD +06 4557	GL792.1A	8.54	900	105
101382	Oct97	195987	BD +41 3799	G209-35	7.09	3600	110
103269	Oct98	...	BD +41 3931	G212-7	10.28	3600	100
104659	Sep94	201891	BD +17 4519	...	7.37	1200	165
104659	Oct97	201891	BD +17 4519	...	7.37	7200	195
104660	Jul98	201889	BD +23 4264	...	8.06	1200	95
105888	Sep94	204155	BD +04 4674	G25-29	8.49	2700	160
105888	Aug98	204155	BD +04 4674	G25-29	8.49	900	110
106947	Sep94	...	BD +22 4454	G126-19	9.51	3600	105
107975	Oct98	207978	BD +28 4215	...	5.52	300	155
109067	Sep94	...	BD +11 4725	G18-28	9.55	3360	80
109390	A98	210295	BD -14 6222	...	9.55	2400	85
109558	Aug98	...	BD +17 4708	G126-62	9.46	1800	105
112796	Oct98	216143	BD -07 5873	...	7.80	1800	145
114271	Aug98	218502	BD -15 6355	...	8.25	900	110
114962	Aug98	219617	BD -14 6437	G273-1	8.16	1200	120
115167	A98	...	BD +02 4651	G29-23	10.21	3600	80
115610	Aug98	...	BD +33 4707	G190-22	9.35	2000	130
115949	Oct98	221170	BD +29 4940	...	7.67	900	110
116082	Oct98	221377	BD +51 3630	...	7.56	900	75
117029	Aug98	222794	BD +57 2787	G241-66	7.14	600	165
117041	Oct98	...	BD -08 6177	G157-93	10.11	3600	85

^aThe complete version of this table is in the electronic edition of the Journal. The printed edition only contains a sample.

TABLE 3. Lines & Oscillator Strengths

Element	λ (Å)	E.P. (eV)	$\log gf$	Source
Fe I	4531.15	1.49	-2.115	Blackwell <i>et al.</i> 1980a
Fe I	4592.66	1.56	-2.409	Blackwell <i>et al.</i> 1980a
Fe I	4595.36	3.29	-1.758	Obrian <i>et al.</i> 1991
Fe I	4602.01	1.61	-3.114	Blackwell <i>et al.</i> 1980a
Fe I	4602.94	1.49	-2.208	Blackwell <i>et al.</i> 1980a
Fe I	4643.46	3.64	-1.147	Obrian <i>et al.</i> 1991
Fe I	4647.43	2.94	-1.351	Obrian <i>et al.</i> 1991
Fe I	4661.97	2.98	-2.502	Obrian <i>et al.</i> 1991
Fe I	4733.60	1.49	-2.947	Blackwell <i>et al.</i> 1980a
Fe I	4736.77	3.20	-0.752	Obrian <i>et al.</i> 1991
Fe I	4786.81	3.00	-1.606	Obrian <i>et al.</i> 1991
Fe I	4789.65	3.53	-0.957	Obrian <i>et al.</i> 1991
Fe I	4800.65	4.12	-1.028	Obrian <i>et al.</i> 1991
Fe I	4859.74	2.86	-0.764	Obrian <i>et al.</i> 1991
Fe I	4871.32	2.85	-0.362	Obrian <i>et al.</i> 1991
Fe I	4872.14	2.87	-0.567	Obrian <i>et al.</i> 1991
Fe I	4890.75	2.86	-0.394	Obrian <i>et al.</i> 1991
Fe I	4891.49	2.84	-0.111	Obrian <i>et al.</i> 1991
Fe I	4918.99	2.85	-0.342	Obrian <i>et al.</i> 1991
Fe I	4939.69	0.86	-3.300	Blackwell <i>et al.</i> 1979a
Fe I	4994.13	0.91	-3.040	Blackwell <i>et al.</i> 1979a
Fe I	5006.12	2.82	-0.615	Obrian <i>et al.</i> 1991
Fe I	5028.13	3.56	-1.122	Obrian <i>et al.</i> 1991
Fe I	5041.07	0.95	-3.086	Obrian <i>et al.</i> 1991
Fe I	5044.21	2.85	-2.017	Obrian <i>et al.</i> 1991
Fe I	5048.44	3.94	-1.029	Obrian <i>et al.</i> 1991
Fe I	5049.82	2.27	-1.355	Obrian <i>et al.</i> 1991
Fe I	5051.64	0.91	-2.755	Blackwell <i>et al.</i> 1979a
Fe I	5068.77	2.93	-1.041	Obrian <i>et al.</i> 1991
Fe I	5079.23	2.20	-2.027	Blackwell <i>et al.</i> 1982b
Fe I	5079.74	0.99	-3.180	Blackwell <i>et al.</i> 1979a
Fe I	5083.34	0.96	-2.918	Blackwell <i>et al.</i> 1979a
Fe I	5123.72	1.01	-3.028	Blackwell <i>et al.</i> 1979a
Fe I	5127.36	0.91	-3.267	Blackwell <i>et al.</i> 1979a
Fe I	5151.92	1.01	-3.282	Blackwell <i>et al.</i> 1979a
Fe I	5191.45	3.03	-0.551	Obrian <i>et al.</i> 1991
Fe I	5198.71	2.22	-2.095	Blackwell <i>et al.</i> 1982b
Fe I	5216.28	1.61	-2.110	Blackwell <i>et al.</i> 1980a
Fe I	5217.39	3.20	-1.162	Obrian <i>et al.</i> 1991
Fe I	5232.94	2.94	-0.057	Obrian <i>et al.</i> 1991
Fe I	5242.49	3.62	-0.967	Obrian <i>et al.</i> 1991
Fe I	5288.53	3.68	-1.508	Obrian <i>et al.</i> 1991
Fe I	5307.37	1.61	-2.947	Blackwell <i>et al.</i> 1980a
Fe I	5332.90	1.55	-2.776	Obrian <i>et al.</i> 1991
Fe I	5379.57	3.68	-1.514	Obrian <i>et al.</i> 1991
Fe I	5501.46	0.95	-3.046	Obrian <i>et al.</i> 1991
Fe I	5506.78	0.99	-2.757	Blackwell <i>et al.</i> 1979a
Fe I	5662.52	4.16	-0.573	Obrian <i>et al.</i> 1991
Fe I	5701.55	2.56	-2.176	Blackwell <i>et al.</i> 1982c
Fe I	5753.12	4.24	-0.688	Obrian <i>et al.</i> 1991
Fe I	5956.70	0.86	-4.565	Blackwell <i>et al.</i> 1979a
Fe I	6065.49	2.61	-1.490	Blackwell <i>et al.</i> 1982c
Fe I	6082.72	2.22	-3.533	Blackwell <i>et al.</i> 1982b
Fe I	6151.62	2.18	-3.259	Blackwell <i>et al.</i> 1982b
Fe I	6173.34	2.22	-2.840	Blackwell <i>et al.</i> 1982b
Fe I	6219.29	2.20	-2.393	Blackwell <i>et al.</i> 1982b
Fe I	6230.73	2.56	-1.241	Blackwell <i>et al.</i> 1982b
Fe I	6246.32	3.59	-0.877	Obrian <i>et al.</i> 1991
Fe I	6252.56	2.40	-1.647	Blackwell <i>et al.</i> 1982b
Fe I	6265.14	2.18	-2.510	Blackwell <i>et al.</i> 1982b
Fe I	6297.80	2.22	-2.700	Blackwell <i>et al.</i> 1982b
Fe I	6322.69	2.59	-2.386	Blackwell <i>et al.</i> 1982b
Fe I	6344.15	2.43	-2.883	Blackwell <i>et al.</i> 1982b
Fe I	6421.36	2.28	-1.987	Blackwell <i>et al.</i> 1982b
Fe I	6430.85	2.18	-1.966	Blackwell <i>et al.</i> 1982b
Fe I	6481.88	2.28	-2.944	Blackwell <i>et al.</i> 1982b
Fe I	6494.99	2.40	-1.233	Blackwell <i>et al.</i> 1982b
Fe I	6498.95	0.96	-4.659	Blackwell <i>et al.</i> 1979a
Fe I	6593.88	2.43	-2.382	Blackwell <i>et al.</i> 1982b
Fe I	6609.12	2.56	-2.652	Blackwell <i>et al.</i> 1982c
Fe I	6750.15	2.42	-2.581	Blackwell <i>et al.</i> 1982b
Fe I	6945.21	2.42	-2.442	Blackwell <i>et al.</i> 1982b
Fe I	6978.86	2.48	-2.460	Blackwell <i>et al.</i> 1982b
Fe I	7723.20	2.28	-3.577	Blackwell <i>et al.</i> 1982b
Fe I	7912.87	0.86	-4.808	Blackwell <i>et al.</i> 1979a
Fe II	4555.89	2.82	-2.19	Blackwell <i>et al.</i> 1980b
Fe II	4576.34	2.84	-2.91	Blackwell <i>et al.</i> 1980b
Fe II	4582.83	2.84	-3.13	Blackwell <i>et al.</i> 1980b
Fe II	4620.52	2.83	-3.23	Blackwell <i>et al.</i> 1980b
Fe II	4635.31	5.96	-1.30	Moity 1983
Fe II	4670.17	2.58	-4.05	Blackwell <i>et al.</i> 1980b
Fe II	4923.92	2.89	-1.31	Moity 1983

TABLE 3. (continued)

Element	λ (\AA)	E.P. (eV)	$\log gf$	Source
Fe II	4993.35	2.81	-3.65	Blackwell <i>et al.</i> 1980b
Fe II	5100.66	2.81	-4.20	Blackwell <i>et al.</i> 1980b
Fe II	5132.67	2.81	-4.01	Blackwell <i>et al.</i> 1980b
Fe II	5197.58	3.23	-2.24	Moity 1983
Fe II	5234.63	3.22	-2.10	Moity 1983
Fe II	5264.79	3.23	-3.02	Blackwell <i>et al.</i> 1980b
Fe II	5325.56	3.22	-3.15	Blackwell <i>et al.</i> 1980b
Fe II	5414.08	3.22	-3.62	Blackwell <i>et al.</i> 1980b
Fe II	5425.46	3.20	-3.19	Blackwell <i>et al.</i> 1980b
Fe II	5991.38	3.15	-3.57	Blackwell <i>et al.</i> 1980b
Fe II	6084.10	3.20	-3.81	Blackwell <i>et al.</i> 1980b
Fe II	6149.25	3.89	-2.75	Blackwell <i>et al.</i> 1980b
Fe II	6247.56	3.89	-2.34	Blackwell <i>et al.</i> 1980b
Fe II	6416.93	3.89	-2.68	Blackwell <i>et al.</i> 1980b
Fe II	6432.68	2.89	-3.57	Blackwell <i>et al.</i> 1980b
Fe II	6456.39	3.90	-2.13	Blackwell <i>et al.</i> 1980b
Fe II	6516.08	2.89	-3.28	Blackwell <i>et al.</i> 1980b
Fe II	7479.70	3.89	-3.71	Blackwell <i>et al.</i> 1980b
Fe II	7711.73	3.90	-2.57	Blackwell <i>et al.</i> 1980b
Li I	6707.76	0.00	hfs	Smith <i>et al.</i> 1998
Na I	4668.57	2.10	-1.41	Snedden <i>et al.</i> 1997
Na I	5682.65	2.10	-0.70	Snedden <i>et al.</i> 1997
Na I	5688.21	2.10	-0.37	Snedden <i>et al.</i> 1997
Na I	5889.96	0.00	hfs	McWilliam 1995b
Na I	5895.94	0.00	hfs	McWilliam 1995b
Na I	6154.23	2.10	-1.56	Snedden <i>et al.</i> 1997
Na I	6160.75	2.10	-1.26	Snedden <i>et al.</i> 1997
Mg I	4703.00	4.33	-0.52	Fuhrmann <i>et al.</i> 1995
Mg I	4730.03	4.33	-2.31	Fuhrmann <i>et al.</i> 1995
Mg I	5172.70	2.70	-0.39	Fuhrmann <i>et al.</i> 1995
Mg I	5183.27	2.70	-0.17	Fuhrmann <i>et al.</i> 1995
Mg I	5528.42	4.33	-0.50	Fuhrmann <i>et al.</i> 1995
Mg I	5711.09	4.33	-1.67	Fuhrmann <i>et al.</i> 1995
Mg I	7387.70	5.75	-1.10	Shetrone 1996
Mg I	7691.57	5.75	-0.80	Shetrone 1996
Al I	6696.03	3.14	-1.57	Shetrone 1996
Al I	6698.67	3.14	-1.89	Shetrone 1996
Al I	7835.32	4.02	-0.71	Shetrone 1996
Al I	7836.13	4.02	-0.55	Shetrone 1996
Al I	8772.88	4.02	-0.38	Shetrone 1996
Al I	8773.91	4.02	-0.16	Shetrone 1996
Si I	5645.66	4.91	-2.14	Garz 1973
Si I	5665.60	4.90	-2.04	Garz 1973
Si I	5684.52	4.93	-1.65	Garz 1973
Si I	5701.12	4.93	-2.05	Garz 1973
Si I	5708.41	4.93	-1.47	Garz 1973
Si I	5772.26	5.06	-1.75	Garz 1973
Si I	5793.08	4.93	-2.06	Garz 1973
Si I	5797.91	4.93	-2.05	Garz 1973
Si I	6142.49	5.62	-1.48	Snedden <i>et al.</i> 1997
Si I	6145.02	5.61	-1.37	Snedden <i>et al.</i> 1997
Si I	6243.82	5.61	-1.27	Snedden <i>et al.</i> 1997
Si I	7034.91	5.87	-0.88	Garz 1973
Ca I	4512.27	2.52	-1.90	Smith & Raggett 1981
Ca I	4578.56	2.52	-0.70	Smith & Raggett 1981
Ca I	5260.39	2.52	-1.72	Smith & Raggett 1981
Ca I	5261.71	2.52	-0.58	Smith & Raggett 1981
Ca I	5581.97	2.52	-0.56	Smith & Raggett 1981
Ca I	5590.12	2.52	-0.57	Smith & Raggett 1981
Ca I	6161.30	2.52	-1.27	Smith & Raggett 1981
Ca I	6166.44	2.52	-1.20	Smith & Raggett 1981
Ca I	6169.04	2.52	-0.80	Smith & Raggett 1981
Ca I	6169.56	2.52	-0.48	Smith & Raggett 1981
Ca I	6455.60	2.52	-1.29	Smith & Raggett 1981
Ca I	6499.65	2.52	-0.82	Smith & Raggett 1981
Ti I	4512.73	0.84	-0.42	Blackwell <i>et al.</i> 1982a
Ti I	4518.02	0.83	-0.26	Blackwell <i>et al.</i> 1982a
Ti I	4548.76	0.83	-0.29	Blackwell <i>et al.</i> 1982a
Ti I	4555.49	0.85	-0.43	Blackwell <i>et al.</i> 1982a
Ti I	4623.10	1.74	+0.166	Blackwell <i>et al.</i> 1986
Ti I	4645.19	1.74	-0.501	Blackwell <i>et al.</i> 1986
Ti I	4656.47	0.00	-1.28	Blackwell <i>et al.</i> 1982a
Ti I	4840.87	0.90	-0.45	Blackwell <i>et al.</i> 1982a
Ti I	4913.62	1.87	+0.216	Blackwell <i>et al.</i> 1986
Ti I	4997.10	0.00	-2.06	Blackwell <i>et al.</i> 1982a
Ti I	5016.16	0.85	-0.51	Blackwell <i>et al.</i> 1982a
Ti I	5064.65	0.05	-0.93	Blackwell <i>et al.</i> 1982a
Ti I	5113.44	1.44	-0.727	Blackwell <i>et al.</i> 1986
Ti I	5145.47	1.46	-0.518	Blackwell <i>et al.</i> 1986
Ti I	5978.54	1.87	-0.440	Blackwell <i>et al.</i> 1986
Ti II	4636.32	1.16	-3.23	Bizzarri <i>et al.</i> 1993
Ti II	4493.52	1.08	-2.83	Bizzarri <i>et al.</i> 1993

TABLE 3. (continued)

Element	λ (Å)	E.P. (eV)	$\log gf$	Source
Ti II	4409.52	1.23	-2.57	Bizzarri <i>et al.</i> 1993
Ti II	4657.20	1.24	-2.32	Bizzarri <i>et al.</i> 1993
Ti II	4444.56	1.08	-2.21	Bizzarri <i>et al.</i> 1993
Ti II	5418.77	1.58	-2.11	Bizzarri <i>et al.</i> 1993
Ti II	4719.52	1.24	-3.28	Bizzarri <i>et al.</i> 1993
Ti II	4708.66	1.24	-2.37	Bizzarri <i>et al.</i> 1993
Ti II	4583.41	1.16	-2.87	Bizzarri <i>et al.</i> 1993
Ti II	4798.53	1.08	-2.67	Bizzarri <i>et al.</i> 1993
V I	4389.99	0.28	+0.235	McWilliam 1995b
V I	4577.18	0.00	-1.05	Beveridge & Sneden 1994
V I	4875.49	0.04	-0.81	Beveridge & Sneden 1994
V I	6090.22	1.08	-0.06	Beveridge & Sneden 1994
V I	6216.37	0.28	-1.07	Beveridge & Sneden 1994
Cr I	5409.79	1.03	-0.715	Blackwell <i>et al.</i> 1984
Cr I	5348.32	1.00	-1.294	Blackwell <i>et al.</i> 1984
Cr I	5345.81	1.00	-0.975	Blackwell <i>et al.</i> 1984
Cr I	5300.75	0.98	-2.129	Blackwell <i>et al.</i> 1984
Cr I	5296.69	0.98	-1.394	Blackwell <i>et al.</i> 1984
Cr I	4651.29	0.98	-1.476	Blackwell <i>et al.</i> 1984
Cr I	4545.96	0.94	-1.379	Blackwell <i>et al.</i> 1984
Cr I	5329.17	2.91	-0.064	Blackwell <i>et al.</i> 1984
Cr I	4789.35	2.54	-0.366	Blackwell <i>et al.</i> 1984
Cr I	4511.90	3.09	-0.343	Blackwell <i>et al.</i> 1984
Ni I	4604.99	3.48	-0.250	Wickliffe & Lawler 1997
Ni I	4686.21	3.60	-0.580	Wickliffe & Lawler 1997
Ni I	4953.21	3.74	-0.580	Wickliffe & Lawler 1997
Ni I	4998.22	3.61	-0.690	Wickliffe & Lawler 1997
Ni I	6176.81	4.09	-0.260	Wickliffe & Lawler 1997
Ni I	4904.41	3.54	-0.17	Fuhr <i>et al.</i> 1988
Ni I	4937.34	3.61	-0.39	Fuhr <i>et al.</i> 1988
Ni I	5081.11	3.85	+0.30	Fuhr <i>et al.</i> 1988
Ni I	5084.08	3.68	+0.03	Fuhr <i>et al.</i> 1988
Ni I	5115.39	3.83	-0.11	Fuhr <i>et al.</i> 1988
Ni I	5155.76	3.90	-0.09	Fuhr <i>et al.</i> 1988
Ni I	6175.37	4.09	-0.53	Fuhr <i>et al.</i> 1988
Ni I	6177.25	1.83	-3.50	Fuhr <i>et al.</i> 1988
Ni I	6223.99	4.10	-0.99	Fuhr <i>et al.</i> 1988
Y II	4398.01	0.13	-1.00	Snedden <i>et al.</i> 1996
Y II	4883.69	1.08	+0.07	Snedden <i>et al.</i> 1996
Y II	4900.11	1.03	-0.09	Snedden <i>et al.</i> 1996
Y II	5087.43	1.08	-0.17	Snedden <i>et al.</i> 1996
Y II	5200.42	0.99	-0.57	Snedden <i>et al.</i> 1996
Y II	5205.73	1.03	-0.34	Snedden <i>et al.</i> 1996
Zr II	4208.98	0.71	-0.46	Snedden <i>et al.</i> 1996
Zr II	4317.32	0.71	-1.38	Snedden <i>et al.</i> 1996
Ba II	4554.04	0.00	hfs	McWilliam 1998
Ba II	5853.68	0.60	hfs	McWilliam 1998
Ba II	6141.73	0.67	hfs	McWilliam 1998
Ba II	6496.91	0.60	hfs	McWilliam 1998
Eu II	4129.72	0.00	hfs	McWilliam 1995b
Eu II	6645.13	1.37	hfs	McWilliam 1995b

TABLE 4. Solar Abundance Data^a

[Fe/H] ^b	Li ^c	Na ^d	Mg	Al	Si	Ca	Ti ^b
	V	Cr	Ni	Y	Zr	Ba	Eu
Oct 98, Derived Parameters:							
	$T_{eff} = 5725$, $\log g = 4.3$, $[Fe/H]_{atm} = 0.0$, $\xi = 0.85$ km/s						
-0.03	...	-0.01	0.09	0.12	0.11	-0.02	0.00
	0.01	0.05	0.10	-0.04	0.05	0.04	...
Oct 98, Standard Parameters:							
	$T_{eff} = 5770$, $\log g = 4.44$, $[Fe/H]_{atm} = 0.0$, $\xi = 0.84$ km/s						
0.01	...	-0.05	0.05	0.08	0.08	-0.05	0.01
	0.03	0.05	0.07	-0.02	0.07	0.14	...
May 99, Derived Parameters:							
	$T_{eff} = 5750$, $\log g = 4.4$, $[Fe/H]_{atm} = 0.0$, $\xi = 0.80$ km/s						
0.03	...	-0.02	-0.01	0.00	0.02	-0.07	-0.04
	-0.03	0.00	0.01	-0.10	0.09	-0.03	-0.04
May 99, Standard Parameters:							
	$T_{eff} = 5770$, $\log g = 4.44$, $[Fe/H]_{atm} = 0.0$, $\xi = 0.84$ km/s						
0.03	...	-0.01	-0.01	0.00	0.02	-0.07	-0.03
	-0.01	0.00	0.01	-0.10	0.09	-0.03	-0.02
Combined Data, Derived Parameters:							
	$T_{eff} = 5750$, $\log g = 4.4$, $[Fe/H]_{atm} = 0.0$, $\xi = 0.80$ km/s						
0.02	...	-0.03	0.00	0.03	0.05	-0.06	-0.04
	-0.01	0.02	0.03	-0.08	0.09	0.00	-0.06
Combined Data, Standard Parameters:							
	$T_{eff} = 5770$, $\log g = 4.44$, $[Fe/H]_{atm} = 0.0$, $\xi = 0.84$ km/s						
0.02	...	-0.01	0.02	0.05	0.07	-0.04	0.01
	0.03	0.04	0.05	-0.06	0.08	0.00	-0.05

^aAverage values given for stars with multiple observations.

^bAverage value of neutral and ionized species.

^c $\log \epsilon(\text{Li})$

^d $[X/Fe]$ given for all elements except Fe and Li.

TABLE 5. Parameters for Survey Stars^a

HIP	HD/BD	T_{eff} init. (K)	log g init.	T_{eff} atm. (K)	log g atm.	[Fe/H] atm.	ξ atm. (km/s)
...	SUN	5770	4.4 ^b	5750	4.4	+0.0	0.80
171	224930	5359	4.4	5275	4.1	-0.9	1.05
2413	2665	4809	1.7	5050	2.2	-1.8	1.60
3026	3567	5966	4.1	5950	3.9	-1.2	1.40
3086	3628	5578	3.9 ^b	5700	4.1	-0.1	1.00
3554	4306	4809	2.9	4800	1.7	-2.8	1.40
5336	6582	5272	4.5	5250	4.4	-0.8	0.90
5445	6755	4996	3.0	5150	2.8	-1.4	1.50
5458	6833	4365	1.5	4450	1.4	-0.9	1.55
6710	8724	4315	1.9	4625	1.2	-1.7	1.95
7217	9430	5819	4.4	5550	4.2	-0.3	0.70
10140	+29 366	5680	4.3	5425	4.1	-1.0	0.85
10449	-1 306	5670	4.4 ^b	5650	4.4	-0.8	1.00
11349	15096	5126	4.4	5375	4.3	-0.2	0.80
11952	16031	6054	4.2	6100	4.2	-1.6	0.95
12306	16397	5654	4.2 ^b	5650	4.1	-0.5	1.05
13366	17820	5688	4.1 ^b	5700	4.2	-0.7	0.95
14086	18907	5072	3.5 ^b	5075	3.6	-0.6	1.10
14594	19445	5947	4.2	5825	4.2	-2.0	1.10
15394	20512	5022	3.5	5150	3.4	-0.2	1.00
16214	21581	4702	2.6	4825	2.0	-1.6	1.45
17085	22785	6100	4.5 ^b	6500	4.2	-0.1	1.70
17147	22879	5800	4.3 ^b	5800	4.3	-0.8	1.10
17666	23439	5090	4.4	5050	4.5	-0.8	0.60
18235	24616	4958	3.1 ^b	4950	3.2	-0.6	0.90
18915	25329	4672	4.8 ^a	4700	4.8	-1.7	1.35
18995	25532	5094	2.6	5525	2.2	-1.1	2.05
19007	25673	5200	4.7:	5150	4.5	-0.5	1.20
19378	26297	4402	0.7	4500	1.2	-1.6	1.70
19797	284248	6077	4.3 ^b	6025	4.2	-1.5	1.05
21000	+4 701	5850	4.5:	6200	4.1	+0.0	1.40
21586	+50 1021	5675	4.9:	4850	4.1	-0.8	0.25
21609	29907	5228	4.0:	5200	3.8	-1.6	1.55
21648	29574	4100	0.0	4300	0.4	-1.7	1.70
21767	280067	5850	4.9:	5650	4.5	-0.3	0.70
22246	+45 983	5232	5.0:	5200	4.5	-0.2	1.20
22632	31128	5822	4.5 ^b	5825	4.3	-1.4	1.35
23344	+3 740	6072	4.2	6075	3.8	-2.7	0.30
24316	34328	5730	4.5 ^b	5725	4.4	-1.5	1.30
26688	37792	6400	4.3 ^b	6500	4.1	-0.5	1.50
27654	39364	4526	2.2 ^b	4550	2.1	-0.8	1.50
28188	40057	6200	4.6 ^b	6175	4.6	-0.5	1.25
29759	+37 1458	5416	3.3	5200	3.0	-2.0	1.25
29992	44007	4850	2.2	4850	2.0	-1.6	2.20
30668	45282	5162	3.1	5150	3.1	-1.4	1.05
30990	45205	5822	4.0 ^b	5825	4.0	-0.8	1.30
31188	46341	5765	4.3 ^b	5750	4.1	-0.7	1.65
31639	-25 3416	5500	4.6 ^b	5300	4.3	-0.5	0.60
32308	+15 1305	5050	4.9:	5175	4.1	-0.5	1.00
33582	51754	5718	4.3	5725	4.3	-0.5	1.25
34146	53545	6221	4.1 ^b	6300	4.2	-0.3	1.95
34548	53871	6300	4.4 ^b	6250	4.5	-0.3	1.40
36491	59374	5772	4.4 ^b	5800	4.4	-0.8	1.10
36849	60319	5873	4.2 ^b	5850	4.1	-0.7	1.10
37335	SAO134948	4812	2.6	4850	2.7	-1.1	1.50
38541	64090	5362	4.6 ^b	5300	4.7	-1.7	0.85
38621	63791	4725	1.7	4700	1.7	-1.7	2.25
38625	64606	5073	4.5	5200	4.4	-0.7	0.30
40068	+80 245	5360	3.4	5225	3.0	-1.9	1.35
40778	233511	5889	4.3 ^b	5900	4.2	-1.6	1.20
42592	74000	6036	4.1	6025	4.1	-2.0	1.20
44075	76932	5850	4.1 ^b	5900	4.2	-0.7	1.25
44116	76910	6254	4.3 ^b	6275	4.1	-0.4	1.45
44124	-3 2525	5766	4.4:	5750	3.6	-1.8	0.10
44716	78050	4882	2.0:	5000	2.1	-0.9	1.70
44919	78737	6338	3.8	6350	3.8	-0.5	1.80
47139	83212	4550	1.5	4600	1.3	-1.3	1.80
47640	83888	6400	4.2 ^b	6600	4.4	+0.0	1.50
48146	+09 2242	6100	4.6:	6200	4.6	+0.0	1.05
48152	84937	6181	4.0	6375	4.1	-2.0	0.80
49371	87140	4992	2.9	4950	2.3	-1.8	1.75
50139	88725	5645	4.3 ^b	5600	4.3	-0.7	0.35
50173	88609	4435	0.8	4450	0.6	-2.9	2.55
52771	+29 2091	5727	4.5 ^b	5700	4.5	-1.8	1.30
53070	94028	5958	4.2	5900	4.2	-1.4	1.45
54858	97560	5211	2.3	5250	2.0	-1.0	2.15
55022	97916	6318	4.0	6450	4.2	-0.8	1.80
57265	+26 2251	5876	4.1	5875	4.0	-1.0	1.50
57850	103036	3488	0.2:	4375	0.8	-1.6	2.75
57939	103095	4983	4.6 ^b	4950	4.5	-1.3	0.70
58229	103723	5836	4.2	5875	4.1	-0.8	1.25
58357	103912	4803	2.8	5050	3.4	-0.5	1.20

TABLE 5. (continued)

HIP	HD/BD	T_{eff} init. (K)	log g init.	T_{eff} atm. (K)	log g atm.	[Fe/H] atm.	ξ atm. (km/s)
59109	-4 3208	6181	4.0	5900	3.0	-2.5	0.90
59239	105546	5278	2.2	5125	2.1	-1.4	1.55
59330	105755	5726	4.0 ^b	5750	4.1	-0.6	1.25
59750	106516	6116	4.2	6200	4.4	-0.6	1.10
60551	108076	5750	4.0 ^b	5725	4.4	-0.7	1.05
60632	108177	6019	4.4 ^b	6200	4.4	-1.5	1.35
60719	108317	5158	2.6	5100	2.5	-2.2	1.15
61824	110184	4350	1.0	4400	0.6	-2.3	2.80
62747	111721	4809	2.2	4825	2.2	-1.4	1.45
62882	111980	5548	3.8	5600	3.7	-1.1	0.04
63970	+33 2300	6000	4.7	6075	4.4	+0.0	1.00
64115	114095	4553	2.5	4650	2.4	-0.6	1.10
64426	114762	5841	4.1	5800	4.1	-0.7	1.25
65268	116316	6292	4.2	6250	4.1	-0.5	1.50
66246	118055	4252	0.8	4400	1.0	-1.8	2.55
66509	118659	5389	4.3 ^b	5350	4.2	-0.5	0.60
66665	+13 2698	5644	3.8	5500	3.8	-0.8	1.05
66815	119173	5950	4.5 ^b	5875	4.5	-0.5	0.95
68594	122563	4487	0.8	4425	0.6	-2.6	2.05
68796	123710	5759	4.6 ^b	5725	4.5	-0.4	0.90
68807	122956	4240	1.5	4575	1.1	-1.7	1.90
69746	+9 2870	4318	2.1	4600	1.1	-2.3	1.95
70647	126587	4541	1.7	4675	2.3	-2.8	1.55
70681	126681	5452	4.5 ^b	5450	4.5	-1.1	0.80
71886	129392	6600	4.3 ^b	6400	4.1	-0.3	1.50
71887	129515	6250	4.4 ^b	6100	4.3	-0.4	1.20
71939	129518	6300	4.4 ^b	6300	4.4	-0.2	1.50
72461	+26 2606	5966	4.4	5875	4.1	-2.3	0.40
73385	132475	5555	3.8 ^b	5575	3.6	-1.5	1.35
73960	+30 2611	4033	2.2	4500	1.4	-1.2	2.10
74033	134113	5621	4.0	5675	4.1	-0.7	1.05
74067	134088	5587	4.4 ^b	5575	4.3	-0.8	1.10
74079	134169	5771	3.9 ^b	5825	4.0	-0.7	1.30
74234	134440	4737	4.8 ^b	4750	4.5	-1.4	0.70
74235	134439	4979	4.7 ^b	4850	4.5	-1.4	0.70
76976	140283	5638	3.7 ^b	5650	3.4	-2.4	0.75
77946	142575	6496	3.7	6550	3.6	-0.9	1.65
78640	+42 2667	5949	4.2	5950	4.2	-1.3	1.20
80837	148816	5831	4.1	5800	4.1	-0.7	1.15
81170	149414	4928	4.6	5175	4.7	-1.1	0.30
81461	149996	5661	4.0 ^b	5600	4.1	-0.5	1.20
85007	157466	5851	4.2 ^b	5900	4.2	-0.4	1.20
85378	158226	5627	4.0 ^b	5625	4.0	-0.5	1.10
85757	158809	5437	3.9	5450	3.8	-0.5	1.05
85855	+23 3130	4996	2.9	5000	2.2	-2.6	1.40
86013	159482	5654	4.3 ^b	5750	4.4	-0.7	1.15
86431	160693	5654	4.2 ^b	5675	4.1	-0.5	1.15
86443	+2 3375	5775	4.2	5950	3.9	-2.2	1.00
87693	+20 3603	6219	4.0	6175	4.0	-2.0	0.90
88010	163810	5133	4.2	5200	4.0	-1.4	0.70
88039	163799	5758	4.0 ^b	5700	4.0	-0.8	1.30
91058	171620	5962	4.0 ^b	6025	4.1	-0.4	1.40
92167	175305	4936	2.5 ^b	4575	2.4	-1.3	1.40
92532	174912	5765	4.3	5825	4.3	-0.4	1.00
92781	175179	5563	4.1 ^b	5650	4.2	-0.6	0.95
94449	179626	5570	3.7	5625	3.7	-1.2	1.15
96115	338529	6144	3.9	6100	3.6	-2.3	0.80
96185	184499	5601	3.9 ^b	5700	4.1	-0.4	1.00
97023	186379	5688	3.8 ^b	5800	3.8	-0.3	1.30
97468	187111	4337	1.3	4450	1.1	-1.6	1.90
98020	188510	5474	4.6 ^b	5325	4.6	-1.6	1.10
98532	189558	5563	3.7 ^b	5550	3.6	-1.1	1.30
99423	+23 3912	5723	4.0	5650	3.8	-1.4	1.30
99938	192718	5661	4.2 ^b	5650	4.0	-0.6	1.20
100568	193901	5745	4.6 ^b	5650	4.4	-1.0	1.10
100792	194598	5947	4.3 ^b	5875	4.2	-1.1	1.40
101346	195633	5915	3.7	6000	3.9	-0.5	1.40
101382	195987	5150	4.3 ^b	5125	4.0	-0.5	0.40
103269	+41 3931	5445	4.7 ^b	5300	4.6	-1.7	0.85
104659	201891	5889	4.2 ^b	5825	4.3	-1.0	1.00
104660	201889	5533	4.0	5500	3.9	-0.8	1.15
105888	204155	5730	4.0 ^b	5700	4.0	-0.6	1.00
106947	+22 4454	5129	4.4 ^b	5200	4.3	-0.5	1.00
107975	207978	6200	3.8 ^b	6275	3.9	-0.5	1.50
109067	+11 4725	5318	4.7	5300	4.3	-0.8	0.85
109390	210295	4568	2.4	4800	2.2	-1.2	1.50
109558	+17 4708	5898	4.1	6025	4.0	-1.5	1.10
112796	216143	4472	1.7	4525	1.0	-2.1	2.85
114271	218502	6063	4.1 ^b	6200	4.1	-1.7	0.90
114962	219617	5898	3.9	5825	4.3	-1.4	1.40
115167	+02 4651	5932	3.4	6100	3.8	-1.5	1.15
115610	+33 4707	4600	4.3 ^b	4800	4.1	-0.5	1.20

TABLE 5. (continued)

HIP	HD/BD	T_{eff} init. (K)	$\log g$ init.	T_{eff} atm. (K)	$\log g$ atm.	[Fe/H] atm.	ξ atm. (km/s)
115949	221170	4174	1.3	4500	0.9	-2.1	2.75
116082	221377	6460	3.7	6275	3.7	-0.7	1.60
117029	222794	5458	3.8 ^b	5425	3.8	-0.7	1.05
117041	-8 6117	5332	4.2	5300	4.2	-0.8	0.90
Starts from Stephens (1999)							
...	G97-40	5460	4.55	5375	4.7	-1.4	0.80
...	G110-43	5670	4.00	5550	4.4	-2.0	1.60
...	G88-42	5200	4.15	5175	4.5	-1.6	0.30
...	G90-36	5280	3.95	5325	4.3	-1.6	1.10
...	G114-42	5720	4.30	5700	4.6	-0.9	0.95
...	G116-53	5780	4.60	5600	4.5	-1.0	0.90
...	G197-30	5140	4.90	5125	5.0	-1.5	0.80
...	G166-37	5400	4.75	5300	4.8	-1.2	0.60
74419	G15-13	5070	4.50	5075	4.8	-1.5	0.50
...	G16-25	5520	4.35	5400	4.6	-1.7	1.30
...	G93-1	5470	4.30	5450	4.7	-1.4	0.70

^aThe complete version of this table is in the electronic edition of the Journal.
The printed edition only contains a sample.

^bStars used in Figure 6(b).

TABLE 6. Derived Abundances^a

HIP	[Fe/H] ^b	Li ^c V	Na ^d Cr	Mg Ni	Al Y	Si Zr	Ca Ba	Ti ^b Eu
Sun	0.02	...	-0.03	0.00	0.03	0.05	-0.06	-0.04
171	-1.00	-0.01	0.02	0.03	-0.08	0.09	0.00	-0.06
		...	0.26	0.55	0.52	0.42	0.38	0.29
2413	-1.96	0.19	0.09	0.08	-0.06	0.05	-0.19	0.34
		1.22	-0.33	0.25	...	0.42	0.26	0.20
3026	-1.32	-0.06	-0.08	-0.08	-0.51	-0.19	-0.19	...
		2.30	-0.17	0.27	...	0.34	0.33	0.31
3086	-0.17	0.09	-0.01	-0.05	-0.06	0.23	0.15	...
		...	0.02	0.23	0.14	0.18	0.05	0.15
3554	-2.92	-0.05	0.06	0.02	-0.05	-0.07	-0.02	0.20
		0.89	0.39	0.76	0.59	0.41
5336	-0.98	...	-0.12	0.01	-0.35	-0.03	-0.93	...
		...	0.07	0.47	0.41	0.41	0.28	0.34
5445	-1.58	0.13	0.02	0.08	0.04	0.22	-0.12	0.51
		1.05	-0.33	0.26	...	0.30	0.27	0.24
5458	-1.04	-0.05	-0.07	-0.09	-0.22	0.08	0.03	0.65
		...	-0.06	0.45	0.16	0.33	0.37	0.12
6710	-1.83	-0.03	-0.00	0.02	-0.21	0.48	0.08	0.56
		...	-0.06	0.54	0.12	0.50	0.41	0.20
7217	-0.48	-0.04	-0.05	0.01	-0.18	0.11	-0.03	0.41
		...	-0.01	0.32	0.25	0.26	0.16	0.25
10140	-1.14	0.10	0.07	0.06	-0.06	-0.01	-0.07	...
		1.38	0.07	0.41	0.32	0.34	0.25	0.20
10449	-0.98	-0.04	0.00	0.05	-0.21	0.11	-0.04	...
		...	-0.04	0.42	0.33	0.34	0.28	0.30
11349	-0.29	0.08	0.08	0.01	0.08	0.25	0.10	...
		...	0.04	0.21	0.19	0.08	0.09	0.13
11952	-1.71	0.12	-0.01	-0.00	1.02	1.00	0.96	0.30
		2.27	-0.09	0.50	...	0.33	0.38	0.41
12306	-0.63	...	-0.03	-0.05	-0.01	-0.37	0.23	...
		...	0.10	0.31	0.25	0.27	0.17	0.19
13366	-0.77	0.04	-0.00	0.07	-0.23	-0.09	-0.07	0.11
		...	0.11	0.36	0.35	0.38	0.25	0.31
14086	-0.71	0.07	0.03	0.06	-0.04	0.08	-0.01	0.28
		...	0.11	0.43	0.43	0.38	0.27	0.33
14594	-2.13	0.17	0.04	0.06	0.06	0.38	-0.09	0.39
		2.25	-0.05	0.52	...	0.73	0.35	0.37
15394	-0.30	...	-0.05	0.05	-0.10	...	-0.14	...
		1.34	0.02	0.23	0.25	0.17	0.13	-0.01
16214	-1.74	0.02	0.09	0.14	-0.20	0.00	-0.09	0.03
		0.93	-0.08	0.61	0.21	0.48	0.41	0.32
17085	-0.22	-0.05	-0.08	0.02	-0.08	0.27	0.03	0.51
		...	-0.01	0.01	...	0.20	0.08	...
17147	-0.91	0.13	...	0.00	0.36	...
		1.44	0.08	0.41	0.31	0.35	0.26	0.32
17666	-1.10	0.18	0.03	0.02	0.05	0.27	0.11	...
		...	-0.05	0.46	0.41	0.50	0.29	0.36
18235	-0.72	0.20	0.07	0.05	0.55	0.68	0.44	...
		...	0.01	0.38	0.38	0.34	0.26	0.29
18915	-1.85	0.11	0.04	-0.01	0.24	0.35	0.05	0.34
		...	0.14	0.38	0.47	0.59	0.36	0.35
18995	-1.26	0.09	-0.04	0.07	0.17	0.79	0.11	...
		...	-0.05	0.58	...	0.54	0.27	0.30
19007	-0.62	-0.02	-0.08	0.02	-0.05	0.32	0.51	0.39
		...	0.17	0.20	0.31	0.24	0.18	0.25
19378	-1.73	0.19	...	0.06	-0.07	...
		...	-0.33	0.45	0.15	0.34	0.29	0.30
19797	-1.68	-0.04	-0.08	-0.05	-0.24	0.34	-0.05	0.03
		2.26	0.09	0.34	...	0.19	0.32	0.38
21000	-0.16	...	-0.11	0.00	0.00	-0.01	0.04	...
		...	-0.01	0.08	0.07	0.09	0.07	0.03
21586	-0.91	-0.25	0.04	0.04	0.04	...	0.16	...
		...	0.04	0.31	0.37	0.35	0.26	0.28
21609	-1.76	0.26	0.03	0.09	-0.07	...	-0.17	...
		1.24	-0.25	0.34	0.39	0.63
21648	-1.88	0.05	...	-0.05	-0.30	...
		...	-0.18	0.71	...	0.42	0.36	0.32
21767	-0.44	-0.10	-0.11	-0.09	0.57	...
		...	-0.02	0.31	0.31	0.23	0.12	0.29
22246	-0.38	0.08	0.06	0.04	-0.08	...	-0.02	0.28
		...	0.03	0.41	0.35	0.25	0.03	0.11
22632	-1.59	0.19	-0.08	-0.01	-0.16	...	-0.15	0.57
		2.18	-0.17	0.36	...	0.63	0.36	...
23344	-2.84	0.10	0.00	...
		2.05	-0.20	0.58	0.47	...
24316	-1.71	...	-2.83	-0.50	...
		2.12	-0.25	0.30	...	0.50	0.35	0.45
26688	-0.60	0.11	0.19	...
		...	0.13	0.11	...	0.31	0.15	0.33
27654	-0.94	-0.10	...	0.10	1.29	...
		...	0.30	0.46	...	0.50	0.30	0.24
		-0.00	-0.07	0.10	-0.24	...

TABLE 6. (continued)

HIP	[Fe/H] ^b	Li ^c V	Na ^d Cr	Mg Ni	Al Y	Si Zr	Ca Ba	Ti ^b Eu
28188	-0.62	2.46	0.02	0.04	-0.06	0.13	0.02	0.14
		-0.02	-0.00	-0.03	-0.03	...	0.20	...
29759	-2.17	1.25	-0.04	0.54	0.38	0.18
		0.00	-0.17	-0.04	-0.04	0.35	0.09	...
29992	-1.71	...	-0.08	0.33	...	0.50	0.28	0.25
		-0.03	-0.29	-0.03	-0.27	...
30668	-1.50	...	-0.22	0.25	...	0.32	0.27	0.15
		-0.05	-0.11	-0.07	0.00	...
30990	-0.89	...	0.08	0.33	...	0.36	0.23	0.24
		0.11	-0.04	0.06	-0.07	...
31188	-0.80	...	0.14	0.21	...	0.36	0.16	0.02
		0.15	-0.02	-0.01	-0.15	...
31639	-0.62	...	0.04	0.35	0.36	0.31	0.18	0.27
		0.17	0.03	0.08	-0.15	...	-0.10	0.23
32308	-0.64	...	0.03	0.22	0.21	0.23	0.11	0.01
		-0.03	-0.01	0.08	-0.06	...	0.05	...
33582	-0.74	...	0.06	0.47	...	0.38	0.24	0.41
		...	0.10	-0.18	...
34146	-0.40	2.73	-0.01	0.10	-0.12	0.20	0.07	0.20
		0.12	...	0.08	0.05	0.15
34548	-0.46	2.51	0.08	0.09	0.04	0.15	0.08	0.16
		0.02	0.07	0.03	-0.05	0.06	0.13	0.35
36491	-0.93	1.70	0.09	0.35	0.16	0.33	0.22	0.33
		0.10	0.01	0.04	-0.04	0.18	-0.02	0.31
36849	-0.88	...	0.10	0.31	...	0.29	0.20	0.27
		0.09	0.02	0.05	0.02	...
37335	-1.26	...	0.32	0.63	...	0.64	0.44	0.26
		0.10	-0.05	0.10	0.04	...	-0.02	0.38
38541	-1.79	1.19	-0.13	0.29	...	0.29	0.28	0.28
		0.00	0.02	-0.04	-0.03	0.31	-0.01	0.06
38621	-1.81	...	-0.07	0.43	...	0.54	0.40	0.27
		0.06	-0.28	0.04	-0.33	...
38625	-0.86	...	0.02	0.34	0.28	0.27	0.22	0.28
		0.12	0.04	0.04	0.06	0.21	-0.11	0.29
40068	-2.05	...	-0.50	-0.08	-0.12	-0.20
		...	-0.12	-0.02	-1.87	-1.04
40778	-1.70	2.17	-0.13	0.42	...	0.44	0.37	0.35
		-0.05	-0.09	-0.03	-0.06	...	-0.03	...
42592	-2.08	...	0.23	0.26	0.45	0.20
		...	-0.05	0.04	...
44075	-0.91	...	0.08	0.39	...	0.37	0.31	0.31
		0.11	0.03	0.05	-0.02	...
44116	-0.58	2.33	0.06	0.17	0.03	0.22	0.11	0.08
		0.19	-0.05	0.02	-0.07	-0.07	0.16	-0.04
44124	-1.96	0.37	...	0.37	0.24	0.25
		...	-0.14	0.12	0.10	...
44716	-1.08	...	-0.15	0.36	...	0.35	0.30	0.26
		0.04	-0.06	0.05	0.12	...
44919	-0.65	...	0.19	0.07	...	0.35	0.10	...
		...	-0.06	0.03	...
47139	-1.46	...	-0.18	0.54	...	0.42	0.27	0.29
		-0.06	-0.17	-0.00	0.16	...
47640	-0.08	...	-0.07	-0.02	-0.04	0.06	0.01	0.00
		0.13	0.04	-0.05	0.15	0.07	0.37	0.01
48146	-0.05	2.66	-0.11	-0.08	-0.08	0.02	-0.02	0.13
		0.01	0.01	-0.02	0.08	0.14	0.13	0.20
48152	-2.08	2.40	-0.10	0.35	0.39	0.40
		...	0.01	0.03	0.03	...	0.00	...
49371	-1.95	...	0.16	0.45	...	0.60	0.39	0.41
		-0.03	-0.24	0.10	0.24	...
50139	-0.68	0.32	0.25	0.26	0.19	0.25
		-0.02	0.07	0.04	-0.02	...	0.08	0.46
50173	-3.01	...	0.03	0.49	0.42	0.25
		...	-0.24	-1.01	...
52771	-1.98	...	-0.15	0.38	0.42	0.54
		...	-0.09
53070	-1.55	2.20	0.03	0.53	0.22	0.55	0.38	0.40
		0.03	-0.01	0.08	0.14	...	0.28	0.33
54858	-1.17	...	-0.12	0.21	...	0.42	0.19	0.22
		-0.08	-0.08	-0.07	-0.08	...
55022	-0.90	...	0.19	0.40	...	0.49	0.30	0.44
		...	-0.07	0.05	...
57265	-1.10	...	-0.29	0.19	...	0.19	0.26	0.17
		-0.11	0.01	-0.10	-0.18	0.11	0.01	0.48
57850	-1.78	...	0.13	0.45	0.35	0.49	0.23	0.29
		-0.15	-0.21	-0.11	0.09	...	0.35	...
57939	-1.46	0.42	-0.33	0.29	0.02	0.33	0.30	0.30
		0.08	0.05	-0.06	-0.06	0.50	-0.03	0.72
58229	-0.94	...	-0.14	0.18	...	0.24	0.20	0.20
		-0.14	-0.03	-0.10	-0.15	0.04	0.07	0.32
58357	-0.65	...	0.04	0.31	...	0.32	0.18	0.32
		0.12	-0.05	0.03	0.16	...

TABLE 6. (continued)

HIP	[Fe/H] ^b	Li ^c V	Na ^d Cr	Mg Ni	Al Y	Si Zr	Ca Ba	Ti ^b Eu
59109	-2.62	...	0.34	0.62	0.58	0.54
		...	0.06	...	0.03	0.21	-0.38	...
59239	-1.49	...	0.06	0.56	...	0.47	0.42	0.27
		0.00	0.04	0.00	0.13	...
59330	-0.75	...	0.08	0.27	...	0.33	0.17	0.28
		...	0.01	0.00	0.02	...
59750	-0.78	...	0.17	0.39	0.28	0.53	0.28	0.27
		0.22	0.00	0.05	-0.15	0.05	0.05	0.21
60551	-0.86	...	0.05	0.29	...	0.34	0.25	0.27
		0.08	0.01	0.10	-0.02	...
60632	-1.65	2.42	0.04	0.43	...	0.64	0.36	0.44
		-0.13	-0.02	0.07	0.08	0.28	0.02	...
60719	-2.35	...	0.11	0.49	...	0.43	0.39	0.24
		...	-0.17	...	-0.25	0.27	-0.02	...
61824	-2.44	...	-0.49	0.56	0.42	0.29
		-0.07	-0.24	0.01	-0.18	...	-0.40	...
62747	-1.54	0.85	-0.00	0.56	0.41	0.55	0.40	0.26
		-0.04	-0.04	0.02	-0.00	0.32	0.08	0.26
62882	-1.26	2.17	0.00	0.50	0.44	0.47	0.33	0.27
		-0.03	-0.04	0.05	0.12	0.33	0.22	0.27
63970	-0.09	2.56	-0.08	0.00	-0.04	0.05	0.00	0.04
		0.02	0.05	0.00	0.02	0.00	0.15	-0.06
64115	-0.74	...	0.15	0.47	0.41	0.39	0.27	0.29
		0.22	0.05	0.09	0.04	0.58	-0.01	0.39
64426	-0.82	1.99	0.17	0.43	0.24	0.32	0.20	0.24
		0.11	0.01	0.05	-0.14	0.03	-0.02	0.26
65268	-0.67	2.26	0.14	0.16	0.05	0.26	0.17	0.12
		0.14	0.01	0.02	-0.03	0.02	0.25	0.27
66246	-1.91	...	-0.15	0.44	...	0.41	0.32	0.26
		-0.07	-0.18	-0.02	-0.25	0.17	0.04	0.54
66509	-0.68	...	0.01	0.36	0.28	0.27	0.20	0.19
		0.11	0.03	0.06	-0.16	0.02	-0.07	0.25
66665	-0.97	...	0.16	0.49	0.46	0.42	0.34	0.25
		-0.01	0.05	0.08	-0.10	0.06	-0.06	0.08
66815	-0.64	1.92	-0.02	0.14	0.05	0.17	0.09	0.17
		-0.00	-0.01	-0.02	-0.18	-0.10	0.06	0.22
68594	-2.79	...	0.10	0.63	...	0.42	0.33	0.22
		-0.04	-0.25	0.12	-0.44	-0.08	-1.04	...
68796	-0.52	1.68	0.02	0.09	0.10	0.12	0.06	0.13
		-0.05	0.03	0.02	-0.07	0.04	0.05	0.20
68807	-1.83	...	-0.13	0.49	...	0.40	0.37	0.20
		-0.08	-0.12	-0.03	-0.30	0.27	-0.05	0.40
69746	-2.41	...	-0.03	0.51	...	0.64	0.39	0.29
		-0.08	-0.19	-0.05	-0.43	-0.03	-0.60	...
70647	-2.99	0.77	0.42	0.72	0.41	0.33
		...	-0.28	0.09	-0.12	...	-0.16	...
70681	-1.25	1.23	-0.21	0.31	0.28	0.49	0.31	0.31
		-0.04	0.00	-0.02	0.14	...	0.19	...
71886	-0.40	2.07	0.10	0.12	-0.01	0.19	0.08	0.04
		0.13	0.03	-0.00	-0.07	0.06	0.29	0.28
71887	-0.49	2.58	0.01	0.07	0.04	0.16	0.07	0.06
		-0.00	0.02	-0.00	-0.04	0.04	0.23	0.11
71939	-0.37	2.64	0.09	0.10	-0.01	0.16	0.07	0.11
		0.04	0.03	-0.03	0.01	0.20	0.25	0.16
72461	-2.48	2.13	-0.07	0.42	0.37	0.52
		...	-0.12	-0.32	...
73385	-1.59	2.23	0.00	0.56	...	0.58	0.34	0.29
		-0.09	-0.04	0.06	0.10	0.41	0.22	...
73960	-1.37	...	-0.37	0.27	-0.03	0.25	0.17	0.23
		-0.05	-0.07	-0.14	-0.41	0.33	0.16	0.69
74033	-0.78	1.86	0.13	0.34	0.24	0.32	0.21	0.29
		0.05	-0.02	-0.00	0.07	0.36	0.01	0.30
74067	-0.90	...	0.11	0.38	0.30	0.37	0.24	0.29
		0.03	-0.01	0.06	-0.04	0.00	-0.07	0.50
74079	-0.83	2.32	0.04	0.34	0.28	0.33	0.20	0.26
		0.07	-0.01	0.05	-0.12	0.12	-0.02	0.31
74234	-1.51	...	-0.62	0.06	-0.22	0.20	0.17	0.15
		0.00	-0.00	-0.08	-0.44	...	-0.31	0.40
74235	-1.57	0.36	-0.54	0.07	-0.29	0.18	0.15	0.18
		-0.03	-0.03	-0.10	-0.24	...	-0.27	0.30
76976	-2.51	2.18	0.00	0.47	0.37	0.40
		...	-0.17	0.14	-1.03	...
77946	-0.97	1.45	0.21	0.55	-0.11	0.45	0.36	0.35
		0.15	-0.01	0.09	-0.00	0.09	0.05	0.24
78640	-1.48	2.28	-0.10	0.41	...	0.44	0.38	0.36
		-0.04	-0.04	-0.00	0.09	0.37	0.09	0.44
80837	-0.83	1.82	0.20	0.40	0.32	0.38	0.25	0.31
		0.13	0.09	0.09	-0.09	0.08	-0.02	0.31
81170	-1.26	...	-0.11	0.41	0.20	0.35	0.27	0.39
		0.14	0.06	0.00	0.37	0.64	0.06	0.50
81461	-0.65	...	0.18	0.47	0.39	0.41	0.25	0.30
		0.08	0.07	0.10	-0.01	0.10	0.01	0.55

TABLE 6. (continued)

HIP	[Fe/H] ^b	Li ^c V	Na ^d Cr	Mg Ni	Al Y	Si Zr	Ca Ba	Ti ^b Eu
85007	-0.50	2.31	0.01	0.13	0.02	0.13	0.02	-0.01
		-0.07	-0.03	-0.01	-0.14	-0.04	0.11	-0.04
85378	-0.64	...	0.14	0.43	0.41	0.36	0.27	0.30
		0.24	0.04	0.12	-0.04	0.20	-0.01	0.44
85757	-0.76	...	0.13	0.45	...	0.38	0.39	0.31
		0.06	0.12	0.09	0.12	...	0.09	0.27
85855	-2.70	0.96	-0.09	0.55	0.40	0.23
		-0.08	-0.17	-0.04	...	-0.21	-0.53	...
86013	-0.82	1.15	0.14	0.39	0.37	0.37	0.28	0.34
		0.11	0.03	0.04	-0.00	0.19	-0.07	0.37
86431	-0.64	...	0.08	0.33	0.34	0.29	0.17	0.20
		0.02	0.02	0.01	-0.15	-0.01	-0.07	0.22
86443	-2.32	0.52	0.38	0.42
		...	0.00	0.07	0.07	...	-0.25	...
87693	-2.11	2.30	0.12	0.46	0.39	0.48
		...	-0.05	0.06	-0.46	...
88010	-1.49	1.38	-0.21	0.40	0.17	0.25	0.36	0.18
		-0.01	0.06	-0.03	-0.23	0.24	-0.01	...
88039	-0.96	1.82	0.08	0.42	0.34	0.47	0.32	0.33
		0.10	0.03	0.06	-0.03	0.08	0.00	0.42
91058	-0.54	2.48	0.10	0.21	0.17	0.25	0.11	0.15
		0.08	0.03	0.05	-0.13	0.00	0.06	0.07
92167	-1.47	1.04	-0.11	0.35	0.05	0.39	0.27	0.22
		-0.04	-0.06	-0.07	-0.20	0.16	0.03	0.48
92532	-0.56	2.18	0.06	0.21	0.15	0.22	0.11	0.11
		0.00	0.01	0.04	-0.10	-0.06	0.16	0.16
92781	-0.75	...	0.09	0.37	0.33	0.33	0.26	0.25
		0.09	-0.00	0.04	0.09	-0.04	0.24	0.37
94449	-1.26	1.81	0.12	0.48	0.34	0.43	0.38	0.27
		0.15	0.02	0.02	-0.02	0.21	-0.02	0.47
96115	-2.41	2.16	0.08	0.58	0.51	0.49
		...	-0.05	0.23	0.08	...	-0.16	...
96185	-0.58	1.24	0.19	0.38	0.33	0.32	0.21	0.32
		0.12	0.04	0.06	-0.06	0.09	0.04	0.29
97023	-0.48	2.25	0.08	0.23	0.17	0.19	0.13	0.12
		0.02	0.04	0.05	-0.22	-0.06	0.03	0.10
97468	-1.71	...	0.01	0.57	...	0.44	0.44	0.35
		-0.04	-0.11	0.01	-0.18	...	-0.00	0.27
98020	-1.67	1.41	-0.29	0.26	...	0.36	0.27	0.28
		...	0.04	0.00	-0.05	0.13	-0.11	...
98532	-1.23	2.26	-0.12	0.50	0.26	0.45	0.37	0.31
		0.08	0.00	0.07	0.14	0.39	0.23	0.06
99423	-1.50	2.43	-0.15	0.41	...	0.46	0.38	0.34
		-0.07	-0.05	-0.01	0.02	0.34	0.08	...
99938	-0.74	...	0.18	0.44	0.36	0.37	0.26	0.27
		0.07	0.03	0.11	-0.15	-0.04	-0.05	0.41
100568	-1.17	1.90	-0.31	0.18	-0.12	0.17	0.21	0.20
		-0.16	-0.03	-0.12	-0.11	-0.02	-0.02	0.67
100792	-1.23	2.20	-0.07	0.28	0.06	0.29	0.21	0.22
		0.00	-0.04	-0.01	-0.17	0.18	0.04	...
101346	-0.65	2.34	0.13	0.20	0.12	0.23	0.13	0.14
		0.05	0.01	0.01	-0.15	0.04	0.04	0.09
101382	-0.66	...	0.19	0.44	0.51	0.41	0.26	0.31
		0.23	-0.02	0.12	0.02	...	-0.10	0.29
103269	-1.81	1.34	-0.41	0.29	...	0.32	0.23	0.24
		0.07	-0.06	-0.04	-0.13	0.10	0.00	...
104659	-1.12	2.15	0.08	0.38	0.22	0.36	0.21	0.27
		-0.03	-0.02	0.01	-0.07	0.18	-0.03	0.24
104660	-0.96	...	0.23	0.50	0.41	0.46	0.44	0.31
		0.13	0.05	0.05	-0.01	0.13	0.05	...
105888	-0.75	1.37	0.15	0.45	0.37	0.37	0.27	0.32
		0.11	0.05	0.09	-0.07	-0.02	0.04	...
106947	-0.64	...	0.21	0.40	...	0.35	0.32	0.24
		0.23	0.10	0.14	0.08	...	-0.14	0.63
107975	-0.63	...	0.17	0.27	0.09	0.24	0.14	0.12
		0.13	-0.03	0.06	-0.06	-0.01	0.28	...
109067	-0.97	...	0.03	0.36	...	0.34	0.32	0.25
		0.08	0.04	0.07	0.21	...	-0.10	...
109390	-1.34	0.02	-0.05	0.50	0.26	0.41	0.23	0.29
		-0.07	-0.10	-0.08	0.04	0.29	0.01	0.39
109558	-1.63	2.25	0.00	0.40	...	0.25	0.42	0.42
		0.19	0.00	-0.10	-0.06	0.26	0.09	...
112796	-2.25	...	-0.50	0.35	0.17	0.51	0.29	0.22
		-0.05	-0.15	0.06	-0.20	0.19	-0.48	0.53
114271	-1.80	2.32	0.07	0.33	0.38	0.41
		...	-0.06	0.04	0.07	0.37	-0.03	...
114962	-1.54	2.22	-0.26	0.29	...	0.30	0.33	0.28
		...	-0.02	-0.00	-0.16	0.23	-0.00	...
115167	-1.77	2.36	0.10	0.33	...	0.40	0.43	0.38
		...	-0.03	0.09	-0.05	...	0.13	...
115610	-0.63	...	0.23	0.50	0.57	0.40	0.28	0.22
		0.40	0.05	0.13	-0.07	...	-0.09	0.42

TABLE 6. (continued)

HIP	[Fe/H] ^b	Li ^c V	Na ^d Cr	Mg Ni	Al Y	Si Zr	Ca Ba	Ti ^b Eu
115949	-2.19	...	-0.50	0.46	...	0.54	0.38	0.25
		-0.07	-0.22	0.10	-0.28	0.12	-0.28	0.62
116082	-0.82	...	0.26	0.31	...	0.21	0.18	0.14
		0.05	-0.02	0.07	-0.10	-0.10	0.18	...
117029	-0.81	1.41	0.12	0.42	0.38	0.38	0.25	0.30
		0.05	0.02	0.09	-0.08	0.13	-0.03	...
117041	-0.88	...	0.12	0.53	0.46	0.45	0.32	0.30
		0.19	0.07	0.09	-0.02	0.22	-0.10	...
Stars from Stephens (1999)								
G97-40	-1.57	...	-0.38	0.14	...	0.44	0.28	0.40
		...	0.05	0.00	0.09	...	-0.05	...
G110-43	-2.19	0.41	0.32	0.20
		...	-0.07	0.21	-0.14	...
G88-42	-1.72	...	-0.59	0.18	0.15	0.09
		...	-0.04	-0.16	-0.50	...	-0.08	...
G90-36	-1.75	...	-0.65	0.28	...	0.38	0.29	0.13
		...	0.02	-0.14	-0.20	...	0.06	...
G114-42	-1.12	...	-0.30	0.23	...	0.24	0.19	0.23
		...	-0.02	-0.03	-0.07	...	0.11	...
G116-53	-1.12	...	-0.31	0.08	...	0.22	0.18	0.17
		...	-0.02	-0.07	-0.16	...	0.11	...
G197-30	-1.69	...	-0.56	0.12	0.12	0.30
		...	0.12	0.15	-0.47	...	0.00	...
G166-37	-1.40	...	-0.46	0.10	...	0.14	0.12	0.25
		...	-0.01	-0.12	0.10	...	0.07	...
G15-13	-1.69	...	-0.72	0.09	...	0.27	0.22	0.27
		...	0.06	-0.12	-0.02	...	0.12	...
G16-25	-1.82	...	-0.54	0.11	0.17	0.20
		...	-0.07	-0.15	-0.04	...	-0.06	...
G93-1	-1.58	...	-0.19	0.27	...	0.51	0.20	0.27
		...	-0.03	-0.07	-0.19	...	-0.15	...

^aThe complete version of this table is in the electronic edition of the Journal.
The printed edition contains only a sample.

^bAverage value of neutral and ionized species.

^c $\log \epsilon(\text{Li})$

^d $[\text{X}/\text{Fe}]$ given for all elements except Fe and Li.

TABLE 7. Random Uncertainties in Abundances

Species	σ_{rand}	$\sigma_{[X/H]}$	$\sigma_{[X/Fe]}$
Fe I	0.063	0.074	
Fe II	0.074	0.086	
$\langle Fe \rangle$		0.079	
Li I		0.126	0.100
Na I	0.063	0.100	0.103
Mg I	0.087	0.092	0.070
Al I	0.087	0.092	0.094
Si I	0.059	0.064	0.072
Ca I	0.063	0.077	0.073
Ti I	0.055	0.080	
Ti II	0.056	0.085	
$\langle Ti \rangle$			0.087
V I	0.122	0.136	0.129
Cr I	0.057	0.075	0.075
Ni I	0.062	0.070	0.068
Y II	0.059	0.072	0.064
Zr II	0.098	0.118	0.113
Ba II	0.086	0.119	0.117
Eu II	0.096	0.100	0.105
			σ_{ratio}
[Na/Mg]			0.119
[Y/Zr]			0.125
[Ba/Eu]			0.140
$[\alpha/Fe]$			0.119

TABLE 8. Parametric Sensitivities in Abundances

	T_{eff}		log g		$[\text{Fe}/\text{H}]_{atm}$		ξ		All Vary	
	+150 K	-150 K	+0.2	-0.2	+0.3	-0.3	+0.3	-0.3	+150 K	-150 K
[Fe I/H]	+0.14	-0.15	-0.01	+0.01	-0.01	+0.00	-0.05	+0.06	+0.14	-0.15
[Fe II/H]	-0.02	+0.02	+0.08	-0.07	+0.04	-0.03	-0.03	+0.04	+0.13	-0.12
[Fe/H]	+0.06	-0.06	+0.03	-0.03	+0.02	-0.01	-0.04	+0.05	+0.13	-0.13
log $\epsilon(\text{Li})$	+0.10	-0.11	+0.00	+0.00	+0.00	+0.00	+0.00	+0.00	+0.10	-0.11
[Na/Fe]	+0.07	-0.10	-0.07	+0.07	-0.04	+0.03	+0.00	-0.01	-0.06	+0.04
[Mg/Fe]	+0.02	-0.03	-0.07	+0.06	-0.02	+0.02	+0.01	-0.01	-0.09	+0.09
[Al/Fe]	+0.01	-0.01	-0.05	+0.05	-0.04	+0.04	+0.05	-0.05	-0.12	+0.12
[Si/Fe]	-0.02	0.03	-0.02	+0.02	-0.01	+0.01	+0.04	-0.04	-0.07	+0.07
[Ca/Fe]	+0.04	-0.05	-0.05	+0.05	-0.03	+0.02	+0.01	-0.02	-0.06	+0.05
[Ti I/Fe]	+0.11	-0.13	-0.05	+0.03	-0.04	+0.03	+0.01	-0.01	+0.02	-0.04
[Ti II/Fe]	-0.02	0.03	+0.03	-0.04	+0.02	-0.02	+0.01	-0.01	+0.04	-0.04
[V/Fe]	+0.14	-0.17	-0.03	+0.04	-0.05	+0.04	+0.02	-0.02	+0.05	-0.08
[Cr/Fe]	+0.10	-0.12	-0.05	+0.05	-0.03	+0.02	-0.01	+0.00	+0.01	-0.03
[Ni/Fe]	+0.02	-0.03	-0.04	+0.03	-0.02	+0.01	+0.01	-0.02	-0.04	+0.03
[Y/Fe]	-0.01	+0.02	+0.04	-0.03	+0.03	-0.03	+0.00	+0.02	+0.07	-0.06
[Zr/Fe]	-0.01	+0.01	+0.03	-0.03	+0.03	-0.02	+0.01	+0.00	+0.07	-0.06
[Ba/Fe]	+0.03	-0.03	+0.00	-0.01	+0.03	-0.02	-0.04	+0.03	+0.05	-0.05
[Eu/Fe]	-0.02	+0.07	+0.04	-0.04	+0.05	-0.01	+0.05	-0.05	+0.06	-0.06